

**RELEASING THE BRAKES: STRATEGIES TO REMODEL THE TUMOR
ENVIRONMENT, INCREASE IMMUNE INFILTRATE, AND INDUCE TUMOR
CELL DEATH**

by

Brian J. Francica

**A dissertation submitted to Johns Hopkins University in conformity with the
requirements for the degree of Doctor of Philosophy**

Baltimore, Maryland

June, 2016

ABSTRACT

The tumor immune infiltrate and tumor cytokine microenvironment have been shown to be crucially important to patient responses to immunotherapy. The presence of effector T cells in the tumor correlates highly with good disease prognosis, while the presence of regulatory and inhibitory cell subsets and cytokines predicts poor outcomes. Thus, the ability to manipulate the cellular infiltrate and cytokine presence within the tumor microenvironment (TME) represents an important step forward in initiating productive responses against tumors. Here we employ several vaccination strategies and molecular methods to activate anti-tumor immunity, increase tumor immune infiltration, and skew the cytokine environment of tumors, all with the goal of creating durable and curative immune responses. We show that an attenuated strain of *Listeria Monocytogenes* (LM), engineered to express the tumor antigens TRP-2 and GP-100, has moderate efficacy in activating lymphocytes, increasing immune infiltrate, and reducing tumor burden. However, when this vaccine is combined with the checkpoint blockade antibody aCTLA4-IgG2a, immune infiltration and tumor control increases greatly. These effects are dependent on the ability of aCTLA4-IgG2a to bind Fc receptors and reduce the percentage of CD4⁺ cells that are FoxP3⁺. Lastly, we utilize the the STING agonist ADU-S100, a modified cyclic-di-adenosine molecule, henceforth referred to as cyclic dinucleotide (CDN), to induce innate effector cytokines like GM-CSF, IL-1b, IFN β , and TNF α . Intratumoral administration of CDN leads to TNF α -dependent tumor necrosis and clearance of established tumors. We explore the acute mechanism of CDN action and find that both immune and stromal cells play critical functions by sensing STING, producing cytokines, and modulating the tumor microenvironment. Interestingly, stromal

cell CDN sensing seems to be indispensable for achieving acute tumor necrosis by CDN injection. All of the above methods represent potential clinical targets to manipulate the TME and increase immune infiltrate to achieve better responses, and the underlying molecular mechanisms are important to understand as we go forward exploring the next generation of therapeutic targets and vaccines.

Thesis Committee

Charles G. Drake, MD, PhD, (Primary Thesis Advisor)

Drew M. Pardoll, MD, PhD, (Thesis Advisor)

Stephen B. Baylin, MD

Andrea L. Cox, MD, PhD

Edward W. Harhaj, PhD

Thesis Readers

Charles G. Drake, MD, PhD

Fan Pan, PhD

PREFACE

The following body of work represents an attempt to more fully understand the mechanisms behind a few important cellular and molecular components of the immune system as they pertain to tumor immunology. It was performed not only over the course of many years, but over the course of maturation from student to scientist. With these experiments, comes the full understanding of legitimate differences between mouse and human systems, but also with the knowledge that a greater understanding of the former leads to the ability to translate to the later. The joy of scientific research is the ability to ask an important question at the beginning of the day, and by the end of the day answer it of your own volition. The difficulty of research is spending months or years dedicating your time and emotion into answering questions, only to come up with dissatisfying answers. Both have happened over the course of these projects, but never once will I say it wasn't worth it.

DEDICATION

As I have discovered over the past 5 years, there are many factors that play a part in earning a Ph.D. and writing a thesis. My own volition was but a small part. This thesis is dedicated foremost to my family, without whom I would not have the drive for excellence. From an early age, my parents demanded I strive to exceed in academic areas, and that has made all the difference. To my brothers, our closeness has been a great comfort, your ridiculous achievements have set a high bar for me to look up to, and particularly to Joe, who introduced me to the idea and field of medical research. Lastly, to my friends, without whose support and distraction I would have surely burnt out or gone insane.

ACKNOWLEDGMENTS

Firstly, I would like to thank Dr. Charles G. Drake (Chuck), whose guidance, patience, and expertise, and of course funding made this thesis possible. Chuck is a passionate scientist and physician whose intelligence and insight is only surpassed by his easygoing mentality and friendliness. Through his example, I have learned look for the pith of any scientific enigma, and to have a keen understanding of scientific process. Above all, Chuck has helped me gain an understanding of the process by which basic scientific knowledge can be translated to and utilized by the clinical sphere.

Secondly, I must thank Dr. Drew Pardoll for his time, advice, and willingness to work with me. When I came in as a first year student, without question Drew took me under his council and talked at length with me about the state of the field, potential projects, and how to succeed as a graduate student. Over the years, his guidance and intuition for the future of the field has pointed me in the direction of success, and also the means to achieve it.

I cannot fail to mention Dr. Tim Bullock, my first scientific mentor. Tim is truly one of the more intelligent and well read individuals I have ever met, and learning in his shadow, as well as being consistently outwitted by the enormity of his knowledge proved to be a huge motivation for me to learn more, work harder, and be the best scientist possible. Thank you for taking me under your wing, and I truly apologize for the mess of a lab notebook I left you. The first try at anything is always the roughest.

Thank you to my predecessors in the lab, my current colleagues, and all the students currently training. The lab environment that we have worked to create and have

maintained over the years is extremely rare. An environment where everyone is welcome, and where everyone can be friends, joke around, and advise each other, all with a pipette in hand and music playing.

Importantly, this work would have not been possible without the collaborative, intellectual, and monetary support by our collaborators in biotech, Alan Kormann and Mark Selby from Bristol-Myers Squibb, and Tom Dubensky, Sarah McWhirter, Kelsey Gauthier, Pete Lauer, David Kanne, Laura Hix Glickman, and all of the team from Aduro Biotech. These groups provided not only reagents, but also great conversation and debate that furthered our scientific discovery.

Finally, as above in my dedication, I would like to thank my family for their steadfast support of me and my education, as well as their patience with me through a time that I matured as a scientist and as an individual. Also to my friends, who understand that the balance to working 70 hour weeks is almost always a beer and ultimate frisbee.

TABLE OF CONTENTS

ABSTRACT	ii
PREFACE	iv
DEDICATION	v
ACKNOWLEDGMENTS	vi
TABLE OF CONTENTS.....	viii
LIST OF FIGURES	ix
CHAPTER I: Introduction	1
CHAPTER II: General Materials and Methods	10
CHAPTER III: Combination Listeria + Checkpoint blockade effectively reduces Tumor burden of established B16F10 Melanoma IN a CD8 Dependent manner	16
CHAPTER IV: Combination Listeria + Checkpoint blockade dramatically changes the tumor infiltrate and cytokine microenvironment	27
CHAPTER V: Fc Gamma receptors are indispensable for the anti tumor effects of CTLA4 IGG2a	42
CHAPTER VI: Therapeutic Intratumoral Injection of CDN leads to acute rejection of B16F10 Through modulation of the Tumor Microenvironemnt.....	49
CHAPTER VII: TNFa production is necessary for IT CDN related necrosis and is produced by both stromal and bone marrow derived cells	60
CHAPTER VIII: Both Bone marrow and stromal cell signaling are crucial for an IT CDN response.....	71
CHAPTER IX: Conclusion and Discussion	80
REFERENCES	89
CURRICULUM VITAE.....	99

LIST OF FIGURES

Figure 3-1: Engineered <i>Listeria Melanogaster</i> vaccine leads to significant survival advantage when combined with CTLA-4 IgG2a.	24
Figure 3-2: Engineered <i>Listeria Melanogaster</i> vaccine leads to significant survival advantage when combined with CTLA-4 IgG2a.	25
Figure 3-3: CD4 Depletion enhances treatment effect through Treg depletion, but only in the presence of CD8+ cells.	26
Figure 4-1: Lymphocyte and systemic cytokine levels are increased by vaccination+ checkpoint blockade.	35
Figure 4-2: LM vaccination increases peripheral cytokines.	36
Figure 4-3: Tregulatory Cells are effectively depleted with LM and aCTLA-4 (D).	38
Figure 4-4: Effector cell infiltrate is greatly increased with LM+aCTLA-4 vaccination.	40
Figure 5-1: CTLA-4 (D) therapeutic effect is ablated in FcγR-/- mice.	47
Figure 5-2: Outgrowth and Treg Depletion by CTLA-4 (D) are Fc receptor dependent.	48
Figure 6-1: IT CDN treatment leads to tumor regression in B16F10 tumor bearing animals.	56
Figure 6-2: IT CDN changes the tumor immune infiltrate.	57
Figure 6-3: IT CDN changes the tumor draining lymph node immune infiltrate.	58
Figure 6-4: Cytokine concentrations in tumor microenvironment increase after IT CDN.	59
Figure 7-1: TNFα is required for injection site necrosis after IT CDN therapy.	68
Figure 7-2: Tumor outgrowth is enhanced in IFNαR, STING, cGAS, and RAG-/- animals.	69
Figure 7-3: TNFα produced by both bone marrow and stroma aids in clearance of B16F10.	70

Figure 8-1: Tumor necrosis only occurs in mice with STING competent stromal cells.....78

Figure 8-2: APC become activated via direct and indirect mechanisms after IT CDN.....79

CHAPTER I

INTRODUCTION

Tumor immunology, immune editing, and vaccination

Since the late 1800's, anecdotal evidence linking infection and the regression of tumor masses has been recorded. However, in 1891, William Coley, a surgical oncologist, began injecting *Streptococcus* bacteria directly into tumor masses and observed gradual decrease in tumor burden in some masses¹. Coley's basic experiments are the first examples of immunotherapy in humans, but were not understood to be so at the time. Similarly, over the past 50 years, physicians have observed an increase in incidence of cancer in patients who are immunosuppressed. Patients undergoing transplant surgery and kept on immunosuppressive agents, or those with immune suppressive infections like HIV all have higher incidences of cancer^{2,3}. Based on these observations, in the past two decades, dedicated tumor immunologists have begun to study the intricate mechanisms that regulate immune activation and tolerance to bacteria, viruses, parasites, cancers, and indeed any pathogen that threatens the integrity of our body.

The first studies to define immune system's regulation of cancers utilized MCA-induced sarcoma in animals with a competent immune system (WT), or in animals without T cell and B cells (RAG^{-/-}). Once grown, the tumors from WT and RAG^{-/-} mice were reinjected into WT or RAG^{-/-} animals. Interestingly, all tumors grew normally except those raised in a RAG^{-/-} animal and reinjected into a WT animal, which grew a dramatically reduced rate⁴. This experiment highly suggested that tumors raised in animals with an immune system were somehow shaped by the presence of that immune system to escape future encounters, while tumor raised in animals with no immune system encountered no such pressure, and thus were slowed by the immune system when

they experienced it. This work introduced the idea of immune selection and evasion by tumors, and solidified the idea that the immune system plays a key role in the shaping and elimination of cancer.

The most basic tool of an immunologist is the vaccine. A vaccine is quite simply any combination of molecule, compound, or organism that activates the immune system to kill a specific target. These targets molecularly are short amino acid peptides called epitopes, and thus many vaccines consist of two molecular parts, an adjuvant that activates immune cells, and peptide that grants it specificity. Vaccination to elicit an antibody response has been resoundingly successful, as many common vaccines to control viral and bacterial infections like Measles, Tetanus, Polio, and smallpox have virtually eradicated the effects of those diseases or the actual pathogens themselves. Tumor vaccines generally aim to enhance a cellular CD8⁺ response and have shown relatively disappointing clinical efficacy. Thus, the thrust of immune oncology has been to gain a more thorough understanding of the immune system to create successful vaccination strategies in a directed manner.

CD8⁺ T cells and Target Killing

The immune system has many components, both cellular and acellular. The CD8⁺ T cell, or cytotoxic T cell, is capable of recognizing and killing stressed or infected cell in the body through recognition of cognate antigen as presented by the major histocompatibility complex (MHC). Once an immune response is initiated by infection, dendritic cells (DC) migrate from the site of insult to the draining lymph node, where mature CD8⁺ cells await activation. At the immune synapse, the localized area of contact between a dendritic cell and a CD8⁺ cell, there are an abundance of molecules

that have the capability of activating, inactivating, and otherwise shaping that cells activity to a pathogen⁵. Activation molecules on the DC surface like CD80/CD86, CD70, and OX40L bind to their cognate receptors on CD8+ cells (CD28, CD27, and OX40) to initiate downstream activation pathways⁶⁻¹⁰. On the other hand, there are also many markers on dendritic cells that can regulate a t cell response. Molecules like PD-L1 can lead to a dampening of CD8+ activity, and eventually T cell quiescence or exhaustion¹¹⁻¹⁴. This event where a DC activates a CD8+ Tcell is called priming or activation. This initiates a signaling cascades to allow the cell to replicate, become motile, and most importantly, to produce effector cytokines like granzyme B, interferon Gamma, TNFa, and IL-2. Recently it has been suggested that multifunctional T cells, cells that can produce multiple cytokines rather than only one, represent the population of cells that are highly effective at carrying out their function¹⁵. Once a CD8+ cell has become activated by a dendritic cell in the draining lymph node, it then mobilizes to the site of insult.

At this site, in the absence of overwhelming immunosuppressive modulators (see below), the CD8+ cell can begin killing target cells.

T regulatory Cells

The immune system employs several mechanisms to regulate the killing activity of CD8+ cells. The T regulatory cell (Treg), as it's name suggests, develops from the CD4+ T cell lineage and plays an important role in suppressing the activity of CD8+ T cells¹⁶. Treg are defined by the transcription factor FoxP3¹⁷, and by the surface markers CD4 and CD25¹⁸. In the absence of Treg and other immunosuppressive mechanisms, severe autoimmune diseases can occur¹⁹. There are several proposed mechanisms for how

Treg may suppress, including suppressive cytokine generation²⁰, sequestration of activating cytokines²¹, and dendritic cell suppression or inactivation²²⁻²⁴.

Tregulatory cells are generally thought to develop in two different manners. Natural Treg are thought to develop during T cell maturation in the thymus if the T cell recognizes self antigen during what may otherwise be considered negative selection²⁵. Induced Treg may develop in the periphery when they experience TGF- β and retinoic acid during their activation or possibly at any time during a CD4⁺ T cell's life^{26,27}.

Clinically, Tregulatory cells have become the subject of much focus in tumor immunology. The depletion of Tregulatory cells from the tumor microenvironment can aid in the restoration of effective immune mediated killing.²⁸⁻³²

Anergy and Immune checkpoints

The immune system is capable of complete and sterilizing immunity when it detects a foreign pathogen and mounts a response to it. However, due to the potency of the response generated, the immune system also utilizes a variety of mechanisms to prevent the generation of immune responses to self-proteins. One such mechanism, T cell tolerance, is the phenomenon through which self-reactive T cells are regulated, and is largely mediated by the induction of anergy or deletion. While many of the mechanisms that dictate which of these outcomes occur *in vivo* remain unclear, some *in vitro* experimental systems have uncovered several of the requirements for the imposition of anergy, including the absence of costimulatory signals³³ and the expression of checkpoint proteins^{34,35}. Recently, prolonged expression of the intracellular transcription factors EGR2 and EGR3 have been shown to enforce the anergy on CD4⁺ T-cells, supporting the hypothesis that anergy is an independently programmed and maintained state for T cells

³⁶⁻³⁹. Similar to CD4 T-cells, CD8 T cells have also been found to express EGR2 in tolerizing environments, though its exact role in these circumstances is not fully understood.

Immune checkpoint molecules are one class of regulatory molecules that modify Tcell-Tcell interactions, Tcell-APC interactions, and T cell- Target interactions by blocking receptor binding or by preventing downstream signaling through those receptors. One of the hallmark extracellular proteins associated with anergy is Programmed Death 1(PD-1). PD-1 is an inhibitory checkpoint molecule that, upon ligation with its ligands, PD-L1 (B7-H1) and PD-L2 (B7-DC), negatively regulates the function of CD4⁺ and CD8⁺ T-cells ^{40,41}. PD-1 signals through an immunoreceptor tyrosine-based inhibitory motif (ITIM) that results in the recruitment and activation of the phosphatase SHP-2, which in turn, is thought to inhibit TCR signaling through its phosphatase activity⁴². PD-1 ligation has been shown to play a role in T-cell anergy in cancer models, as PD-1 ^{-/-} mice often have reduced tumor burden when compared to their wild type counterparts⁴³. Furthermore, in preclinical models of melanoma, fibrosarcoma, colon carcinoma, breast carcinoma, and several other types of tumors, monoclonal PD-1 blockade results in tumor control and regression^{13,44}. Reduction in tumor burden in these models often correlates with increased tumor infiltration by immune cells along with increased effector cytokine production by CD4⁺ as well as CD8⁺ T-cells. Similarly, blocking PD-1 in the clinic with a monoclonal antibodies directed at either PD-1 or its ligand, PD-L1, has recently been demonstrated to increase overall survival either alone⁴⁵, or in combination with another checkpoint blockade, CTLA-4 ⁴⁶.

Cytotoxic lymphocyte antigen 4, or CTLA-4, is a key negative regulator of immune activation⁴⁷. It prevents B-7:CD28 ligation by binding B-7 with a higher avidity than CD28, thus sequestering it⁴⁸ and CTLA-4 ligation has been shown to prevent cellular proliferation and induce anergy in vivo³⁴. While cell surface expression of CTLA-4 in many cell types is regulated intracellularly, activated T effector cells, Tregulatory cells, and tumor cells may all express surface CTLA-4⁴⁹⁻⁵¹. However, our group and others have shown that Tregulatory cells, especially those infiltrating the tumor, express CTLA4 at 10-100 times the level of other immune cells⁵². CTLA-4 blockade with monoclonal antibodies has shown efficacy in pre-clinical models, perhaps because anti-CTLA4 antibodies have been shown to specifically deplete adoptively transferred tumor Tregulatory cells through antibody dependent cellular cytotoxicity (ADCC)³¹. Interestingly, experimentation examining non-transferred endogenous populations of Treg do not observe a decrease in absolute number, but rather a reduction in Treg as a percent of TIL^{32,52}.

The STING Pathway

The immune system is evolutionarily primed to prevent infection through the possession of receptors for molecules that are common and necessary to viral and bacterial existence and replication. These Pattern Recognition Receptors (PRRs) bind pathogen associated molecular patterns (PAMPs), and are essential to initiate innate immune responses⁵³⁻⁵⁵. The ensuing integration of danger signals into innate immune signal circuits results in downstream transcription of innate effector molecules such as Interferon- β , TNF α , and IL-1⁵⁶. These effector molecules then allow the stromal and

immune cells of the body to respond by a variety of reactions including MHC expression, an unfolded protein response, or apoptosis.

One such receptor for danger signals is cyclic GMP-AMP synthase (cGAS). cGAS catalyzes the conversion of dsDNA into cyclic dinucleotides (CDN)⁵⁷⁻⁵⁹. CDN in turn, bind to an er-resident protein stimulator of interferon Genes (STING)^{60,61}. In the presence of bound CDN, STING dimerizes and phosphorylates the adaptor protein TBK1, which can in turn phosphorylate IRF-3 and initiate the transcription of type 1 interferons⁶¹⁻⁶⁴. Additionally, STING ligation induces NF-kB signaling that leads to the transcription of TNFa.

Evolutionarily, the cGAS-STING pathway may have developed for several reasons. The obligate intracellular bacteria *Listeria Monocytogenes* produces CDN as a natural metabolic byproduct, and sensing of CDN intracellularly allows for more efficient clearance of the infection^{65,66}. More recently, STING has been implicated in the initiation of immune responses to dsDNA viruses such as gamma herpes virus, polio, and HIV^{57,67-73}, and the discovery that CDN can be shared between cells via gap junctions to prevent the spread of virus to neighboring cells solidifies CDN as a major viral defense mechanism^{74,75}. Interestingly, the receptor has also been shown to have immunosuppressive effects through recruitment of tolerogenic mechanisms^{63,76,77}.

Stromal Cells

The innate system is not sourced solely by bone marrow derived cells that do not need to rearrange genome for receptor production and diversity, but also by every cell in the body that is able to sense danger signals and produce cytokines. The vast majority of cells in the body have the ability to recognize cellular damage through nod like receptors,

cytosolic DNA receptors, viral RNA receptors, as well as general mechanisms that allow for a cell to become immunogenic after stress or death⁷⁸. Many of these cells, such as endothelial cells, epithelial cells, and especially pseudo-immune cells like tissue resident macrophages and microglial cells have the capacity to produce immune cytokines after danger signals are sensed⁷⁹⁻⁸¹. In this way, the stroma is perhaps one of the most crucial initiators of anti-tumor immunity and immunity in general.

CHAPTER II

General Materials and Methods

Cell Lines

B16F10 and CT26 were acquired from ATCC (CRL-6475, and CRL-2639 Respectively) and were cultured in Complete RPMI (10%FBS, 100u/ml penicillin, 100ug/ml streptomycin, 250ng/ml amphotericin, 1mM sodium pyruvate, NEAA).

Mice

C57BL/6 mice (6-8 week old female) were purchased from Jackson Laboratories and BL6-CD45.1 mice (6-8 week old female) were purchased from Charles River. FoxP3 DTR mice were a gift from Dr. Drew Pardoll and FcγR^{-/-} (B6.129P2-Fcγ1g^{tm1Rav}N12) breeder mice were purchased from Taconic and bred in Johns Hopkins Facilities. cGAS^{-/-} animals were a gift from Skip Virgin. STING^{-/-} animals are the Golden Ticket strain, and were a gift from Young Kim. Rag2^{-/-} animals were a gift from Jonathan Powell. IFNar^{-/-} (B6.129S2-Ifnar1^{tm1Agt}/Mmjax), TNFa^{-/-} (B6.129S-Tnftm1Gkl/J), and IL-6^{-/-} (B6;129S2-Il6^{tm1Kopf}/J) breeder pairs were purchased from Jackson laboratories and bred in Johns Hopkins Facilities. All mouse procedures were approved by the Johns Hopkins University Institutional Animal Care and Use Committee and were compliant with the Guide for the Care and Use of Laboratory Animals (8th ed. The National Academic Press. 2011).

Chimeric animals were made by irradiating 6-12 week old animals with 2 doses of 6 gy separated by 3 hours. 3 hours after the second dose of irradiation, mice were reconstituted with 5-10 million cells of unirradiated donor bone marrow via tail vein injection and left to rest for at least 6 weeks. All chimeric animals were put on uniprim

feed at least 1 week before irradiation and removed from uniprim feed at least 1 week before tumor challenge.

Antibodies

Therapeutic antibodies aCTLA-4 IgG1 (9D9), aCTLA-4 IgG2a (9D9), aPD-1 (4H2), anti-DT mIgG1 (1D12) and anti-DT mIgG2a (1D12) were acquired in collaboration with Alan Korman and Mark Selby at Bristol-Myers Squibb. Dosing per injection was 200 ug for all antibodies, administered IP in 200ul PBS.

Immunohistochemistry antibodies included CD3 (SP7), ThermoScientific; CD4 (1), SinoBiological; FoxP3(D608R), Cell Signaling.

Flow cytometry staining antibodies included CD4-Pacific orange (RM4-5) Invitrogen; CD4-FITC (GK1.5), CD8-PerCP/Cy5.5 (53-6.7), CD44-Pacific Blue (IM7), CD11b-AlexaFluor700 (M1/70), CD11c-FITC (N418), F4/80-Pe/Cy7 (BM8), CD16.2(FcRIV)-PE (9E9), FoxP3-APC (FJK-16s), CD25-PerCp/Cy5.5 (PC61), CTLA4-PE (UC10-4B9), CD86-PE/Cy5 (GL-1), IFN-gamma-PE/Cy7 (XMG1.2), CD45-BV605 (30-F11), IFN γ -APC(XMG1.2), Gzb-Pacific Blue (GB11), BioLegend; GranzymeB-PE (16G6), CD4-PerCP Cy5.5 (RM4-5), Viability Dye- APC-Cy7, CD8-FITC (53-6.7), CD44-AF700 (IM7), TNFa-PE (MP6-XT22), eBioscience; TNF-APC (MP6-XT22), BD Biosciences; IL-2-PE-CF594 (JES6-5H4), BD Horizon.

Depletion antibodies aCD4 (GK1.5) and aCD8 (2.43) were obtained from Bio X Cell. Dosing for depletion antibodies was 200ug IP in 200ul PBS on day -3,-1, +1 relative to vaccination, then every 7 days thereafter until completion of the experiment.

For CDN studies antibodies used included CD11b-AF700 (M1/70), CD44-Pacific Blue (IM7), CD11c-FITC (N418), CD86-PE (GL-1), CD19 PerCP-Cy5.5 (6D5), Ly6C-BV605(HK1.4), CD45.2- APC (104), IA/IE- PerCP-Cy5.5 (M5/114.15.2), Ly6G- BV421 (1A8), CD16/32-BV510 (93), F4/80-PE-Cy7 (BM8), CD206-BV711 (C068C2), Ly6c-PerCP- Cy5.5 (HK1.4), and CD4- BV605 (GK1.5), Biolegend; NOS2-APC (CXNFT), NK1.1-PE (PK136), and CD8-PE-Cy7 (53-6.7), EBioscience; CD4-Pacific Orange (RM4-5), Life Technologies; CD45.1-FITC (A20) BD Pharmingen.

LM/2a Tumor Outgrowth and Infiltration Studies

5×10^5 B16F10 cells were implanted between the skin and peritoneal cavity on day 0. On day 5, mice were vaccinated via the tail vein with Listeria or given sham treatment. On days 5, 7, and 9, mice were given 200ug (in 200ul PBS) of blockade antibodies or PBS alone. On day 18 mice were sacrificed. Tumor volume was calculated by the following equation: $(\text{Length} \times \text{Width}^2)/2$. Cell number of spleen and lymph node were counted on a hemocytometer while cell numbers of tumor infiltrate were acquired by flow cytometry. For Cytokine intracellular staining, animals sacrificed and tumors were harvested 10 days after implantation. Whole tumor suspension was incubated with PMA and Ionomycin for 4.5 hours. Cells were fixed for 30 minutes in Fixation/Permeabilization buffer by BD Bioscience (Cat. No. 554714 and 554715) before proceeding to stain.

CDN Tumor Outgrowth and Infiltration studies

5×10^5 B16F10 cells were implanted between the skin and peritoneal cavity on day 0. Tumors were monitored until the group average was $\sim 80 \text{mm}^3$ and then treated with 100ug injections of CDN in 40ul PBS or PBS alone every other day for a total of three treatments. For chimera studies, a surplus of mice were implanted tumor, then when tumors were palpable, animals were selected and groups normalized to $\sim 80 \text{mm}^3$. Tumor outgrowth volume was measured by the equation $V = 1/2(\text{width}^2 * \text{length})$. 24 hours after treatment, some mice were sacrificed for tumor infiltrate studies by flow cytometry or for tumor lysate. Tumor lysate was made by resecting tumors and dissociating in Cell Lytic M (Sigma Cat no. C2978) with Protease Inhibitor Cocktail (Sigma S8820).

Cytokine Array

Blood serum was collected by cheek bleed on days 8 and 11, then by incision of the IVC on day 14. Blood sat to clot for 10 minutes then was centrifuged and serum was harvested. The Luminex Biorad Mouse Group 1 23-plex assay (#M60-009RDPD) was conducted following vendor guidelines. Serum samples were diluted 1:4. Standard curves were generated and within the normal ranges expected with the exception of a reduced range for GMCSF. IL-4 was not detected.

Elisa:

Elisas were purchased as kits as follows: Mouse IL-1b/IL-1f2 (Catalog No. MLB00c), Mouse GM-CSF (Catalog No. MGM00), Mouse IL-6 (Catalog No. M6000B), Mouse TNF-a (Catalog No MTA00B) R&D; VeriKine Mouse IFN γ Elisa (Catalog No

42400-2) PBL Assay Science; Mouse Inflammatory Cytokines Multi-analyte ELISArray Kit (MEM004a), Qiagen.

Statistics:

Statistical significance for bar graphs was determined with a one-sided or two-sided non-paired student's T test (*= $P < .05$, **= $P < .001$, ***= $P < .0001$). Statistical significance for Kaplan-Meier survival graphs was determined by Log-Rank Test.

CHAPTER III

Combination Listeria + Checkpoint blockade effectively reduces Tumor burden of established B16F10 Melanoma IN a CD8 Dependent manner

Introduction

At the onset of an immune response, many molecular interactions determine the magnitude and character of the immune response⁸². Immune checkpoints like PD-L1 expressed on dendritic cells, macrophages, and tumor cells, as well as CTLA4, PD-1, and Lag-3 expressed on Tcells, can blunt an immune response through ligation of their cognate receptors^{35,40,83}. This ligation can promote the dephosphorylation of the Tcell receptor signaling complex through the recruitment of phosphatases like SHP-2 or block interactions with costimulatory molecules⁸⁴⁻⁸⁶. Cytokines in the immune microenvironment like TGF- β and IL-10 can also dampen the immune response by activating pathways to suppress production of effector cytokines by Tcells^{87,88}. Tcells activated in, or experiencing these conditions become less effective in their killing functions, adopt a tolerized and anergic phenotype, and thus become unable to control tumor outgrowth⁴³. However, reversal of this suppressive environment is possible through depletion of tolerogenic cell types, checkpoint blockade antibodies, and vaccination^{32,89-91}.

One such vaccine that has gained popularity is engineered attenuated *Listeria Monocytogenes*. Indeed, a combination GVAX+ *Listeria* vaccine showed a survival advantage over GVAX alone in pancreatic cancer patients.⁹² Unaltered, *Listeria* is an obligate intracellular pathogen that preferentially infects liver and can be associated with liver toxicity⁹³. However, with targeted deletion of select genes, attenuated variants of *Listeria* have been generated that offer the same adjuvant activity with dramatically reduced toxicity⁹³. *Listeria* is also unique in its activation of the immune system by its production of the metabolic byproduct cGAMP, a molecule that has recently been

spotlighted for its potential in intratumoral adjuvant therapy^{65,66,94-96}. Additionally, listeria outperforms other engineered vaccine platforms as a stimulator of effective CD8+ t cell responses due to its preferential infection of CD8+ Dendritic cells, that produce soluble factors which lead to antigen specific activation without upregulating the co-inhibitory marker PD-1 (unpublished data). Preclinical models have shown that Listeria or checkpoint blockade can aid in reduction of tumor burden, but our study differs in that we combine two novel strategies (LM-MEL and aCTLA4 IgG2a), observe efficacy in the highly aggressive line B16F10, and gain insights into the mechanism of Treg management^{29,32,97,98}.

Chapter Specific Materials and Methods

Cell Lines

B16F10 and CT26 were acquired from ATCC (CRL-6475, and CRL-2639 Respectively) and were cultured in Complete RPMI (10%FBS, 100u/ml penicillin, 100ug/ml streptomycin, 250ng/ml amphotericin, 1mM sodium pyruvate, NEAA).

Mice

C57BL/6 mice (6-8 week old female) were purchased from Jackson Laboratories and BL6-CD45.1 mice (6-8 week old female) were purchased from Charles River. All mouse procedures were approved by the Johns Hopkins University Institutional Animal Care and Use Committee and were compliant with the Guide for the Care and Use of Laboratory Animals (8th ed. The National Academic Press. 2011).

Antibodies

Therapeutic antibodies aCTLA-4 IgG1 (9D9), aCTLA-4 IgG2a (9D9), aPD-1 (4H2), anti-DT mIgG1 (1D12) and anti-DT mIgG2a (1D12) were acquired in collaboration with Alan Korman and Mark Selby at Bristol-Myers Squibb. Dosing per injection was 200 ug for all antibodies, administered IP in 200ul PBS.

Depletion antibodies aCD4 (GK1.5) and aCD8 (2.43) were obtained from Bio X Cell. Dosing for depletion antibodies was 200ug IP in 200ul PBS on day -3,-1, +1 relative to vaccination, then every 7 days thereafter until completion of the experiment.

LM/2a Tumor Outgrowth and Infiltration Studies

5×10^5 B16F10 cells were implanted between the skin and peritoneal cavity on day 0. On day 5, mice were vaccinated via the tail vein with Listeria or given sham treatment.

On days 5, 7, and 9, mice were given 200ug (in 200ul PBS) of blockade antibodies or PBS alone. On day 18 mice were sacrificed. Tumor volume was calculated by the following equation: $(\text{Length} \times \text{Width}^2)/2$. Cell number of spleen and lymph node were counted on a hemocytometer while cell numbers of tumor infiltrate were acquired by flow cytometry. For Cytokine intracellular staining, animals sacrificed and tumors were harvested 10 days after implantation. Whole tumor suspension was incubated with PMA and Ionomycin for 4.5 hours. Cells were fixed for 30 minutes in Fixation/Permeabilization buffer by BD Bioscience (Cat. No. 554714 and 554715) before proceeding to stain.

Statistics:

Statistical significance for bar graphs was determined with a one-sided or two sided non-Paired students T test (*= $P < .05$, **= $P < .001$, ***= $P < .0001$). Statistical significance for Kaplan-Meier survival graphs was determined by Log-Rank Test.

Results

Combination therapy with LM-M/aCTLA4-IgG2a dramatically reduces B16F10 tumor burden.

Due to promise generated by recent immunotherapy clinical trials, we sought to design a vaccination strategy that affords the best tumor survival advantage in the highly aggressive mouse melanoma model B16F10. We employed a novel vaccine, an engineered listeria monocytogenes bacteria (LM) that expresses two melanoma antigens shared between mouse and human, TRP-2 and GP-100, and combined it with checkpoint blockade antibodies, administered at 0, 48, and 96 hours after vaccination (Figure 3-1a). Administering this vaccine on its own reduced tumor burden in mice somewhat, though not robustly (Figure 3-1b). We hypothesized that addition of checkpoint blockade antibodies would release the immunosuppressive environment of the tumor and aid in tumor clearance. Somewhat surprisingly, PD-1 blockade conferred no significant reduction in tumor burden, so we altered the vaccination strategy to a different checkpoint blockade target, CTLA-4. Previous publications have shown that CTLA-4 blockade enhances T cell activation and may even increase de novo T cell activation⁹⁹. With this knowledge we treated mice with two different aCTLA-4 monoclonal antibodies, aCTLA-4-IgG1 (hereon referred to as non-depleting or ND) and aCTLA-4-IgG2a (hereon referred to as Depleting or D). aCTLA-4 (ND) has relatively little effect with or without the addition of LM vaccination. Alternatively, aCTLA-4 (D) administration greatly reduces tumor burden as a monotherapy and, with the addition of LM, the combination therapy shows remarkable efficacy in this highly aggressive model (Figure 3-1b and Figure 3-2). Eventually, B16F10 tumor bearing animals do succumb to

tumor burden, but the combination therapy of LM/aCTLA-4 (D) roughly doubles the survival time of these animals from ~25 days to ~50 days (Figure 3-2b). We then repeated these experiments in the lymphoma line EL-4 OVA and achieved similar results (Data not shown) EL-4 OVA responds to LM-OVA as a monotherapy with significant but non-curative effects. However, the addition of aCTLA-4 to this therapy results in the depletion of Tregulatory cells from the tumor environment as well as the clearance and long term survival of the majority of these animals.

CD4+ and CD8+ cells are negative and positive regulators of tumor clearance, respectively.

Due to now overwhelming data suggesting that CD8 cells directly kill tumor cells *in vivo*, we depleted CD4+ and CD8+ subsets in mice by administering the antibodies GK1.5 (aCD4) and 2.43 (aCD8) on days -3 and -1 before vaccination, as well as every 7 days thereafter. Administration of these antibodies allows for near complete depletion of T cells to <0.1% by peripheral blood measurement. Depletion of CD8+ cells from the animal dramatically reduces the ability of the combination therapy LM+aCTLA-4 (D) to control tumor (Figure 3-3b). Any remaining vaccination advantage may be due to CD8-effector subsets such as natural killer cells. Surprisingly, depletion of CD4+ cells after combination treatment does not diminish the effect of immune killing, but rather enhances it (Figure 3-3c). This suggests that any enhancement of CD8+ cell killing by CD4+ conventional cells is overshadowed by the effect of more efficient depletion of CD4+ Tregulatory cells by GK1.5. This supports our previous experimentation that has shown the effects of Treg in the tumor to be a main controlling characteristic for tumor

outgrowth. Similarly, tumor outgrowth in mice vaccinated with LM and treated with GK1.5 mirrors tumor outgrowth in mice treated with LM-M and aCTLA-4 (D), reinforcing our hypothesis that the main effect of aCTLA-4 (D) is to effectively deplete tumor infiltrating Treg, and that differences in the treatment effects between IgG1 and IgG2a isotypes are due to differences in the efficiency of Treg depletion. Lastly, administration of both GK1.5 and 2.43 antibody has the same effect as administering 2.43 antibody alone, further suggesting that CD8 mediated killing is essential for tumor regression (Figure 3-3d).

Figure 3-1

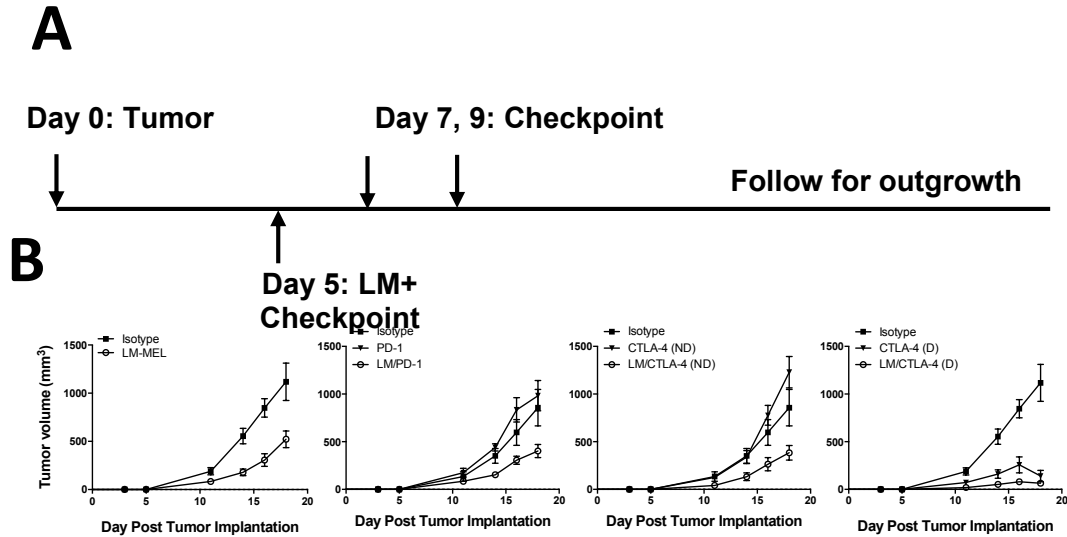


Figure 3-1: Engineered *Listeria Melanogaster* vaccine leads to significant survival advantage when combined with CTLA4- IgG2a. **(A)** Schematic of experimental design. 10^5 B16F10 tumor cells were implanted in the flank of mice on day 0. On Day 5, animals were vaccinated intravenously with LM-MEL. On day 5,7,9, animals were administered checkpoint blockade or isotype control antibodies via IP injection. **(B)** Tumor outgrowth curves of treated animals. Curves are representative of 3 experiments with 5+ animals per experiment.

Figure 3-2

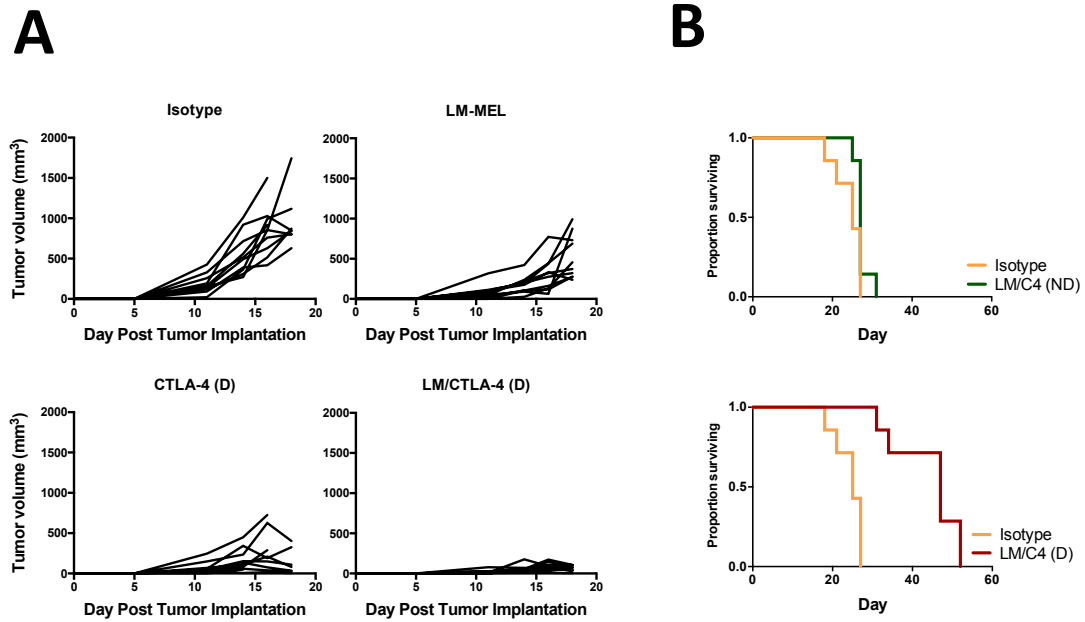


Figure 3-2: Engineered *Listeria Melanogaster* vaccine leads to significant survival advantage when combined with CTLA4- IgG2a. (A) Spaghetti plots of tumor growth in individual mice for the experiment in Figure 3-1. B) Kaplan-Meier curve of mouse survival for experiment in (B). Mice were sacrificed when tumors reached $>2000 \text{ mm}^3$. Curves are representative of 3 experiments with 5+ animals per experiment.

Figure 3-3

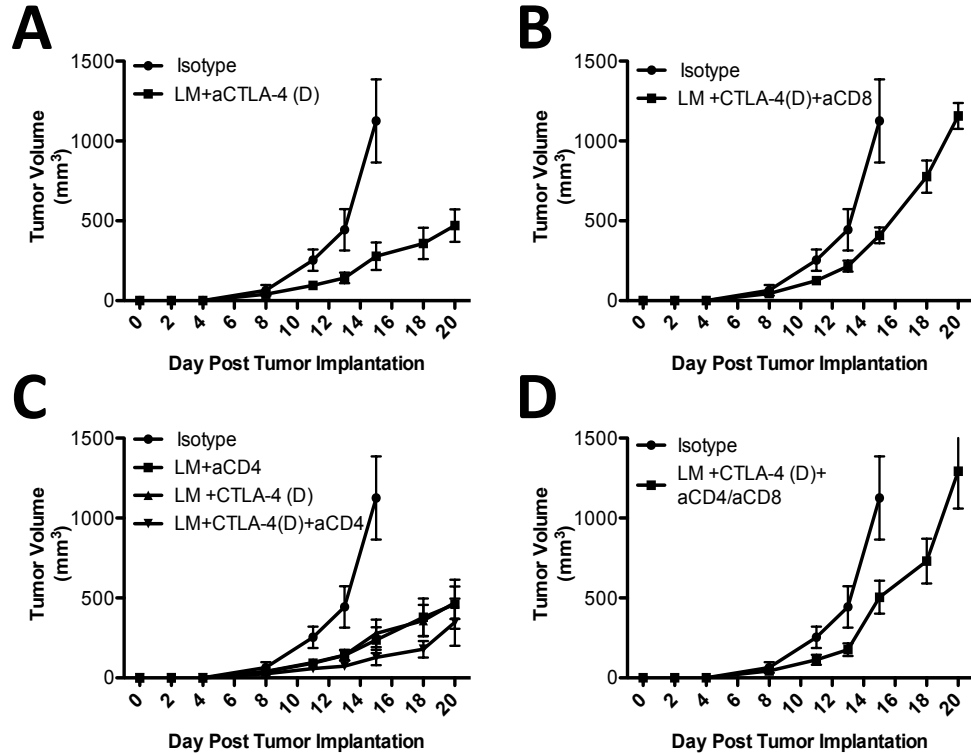


Figure 3-3: CD4 depletion enhances treatment effect through Treg depletion, but only in the presence of CD8⁺ cells. (A-D) Mice were treated with 200ug aCD4(GK1.5), aCD8(2.43), or both antibodies on day -3 and -1 before vaccination/antibody administration (day 2 and 4 after tumor implantation) and continued every 7 days thereafter. LM CTLA4 IgG2a treatment schedule was the same as in Figure 3-1a. Outgrowth was followed until the first tumors reached >2000 mm³. Representative of 1 experiment, 5 mice per group.

CHAPTER IV

Combination Listeria + Checkpoint blockade dramatically changes the tumor infiltrate and cytokine microenvironment

Introduction

The production of cytokines by both immune cells and non-immune stromal cells shapes the tumor micro environment. Recently, the field has come to appreciate that multifunctional t cells, those that produce multiple different cytokines, represent the most effective subset of cells and are not only a good readout for vaccine efficacy, but a good prognosis for tumor clearance. Thus, probing to see if vaccination induces these cells is a major output for therapeutic vaccines. Similarly, analyzing the whole of the tumor microenvironment for cytokine presence allows an understanding of the microenvironment that cells experience while undergoing their functions. Many tumor types, including B16, 4T1, and Her2, have tolerizing tumor microenvironments characterized by the presence of TGF- β and IL-10. Through vaccination, we seek to skew this environment from one of immunosuppression to one of immune activation.

Additionally, the presence and absolute number of infiltrating lymphocytes is crucial for immune clearance of tumors. B16F10 is a relatively uninfiltrated tumor at its basal state, and inducing strong infiltration of lymphocytes into the tumor microenvironment is key to initiating immune mediated killing. Conversely, Tregulatory cells infiltrating in the tumor will prevent the effector function of CD8⁺ T cells, and as such preventing the infiltration and buildup of Tregulatory cells is equally important.

Chapter Specific Material and Methods

Cell Lines

B16F10 and CT26 were acquired from ATCC (CRL-6475, and CRL-2639 Respectively) and were cultured in Complete RPMI (10%FBS, 100u/ml penicillin, 100ug/ml streptomycin, 250ng/ml amphotericin, 1mM sodium pyruvate, NEAA).

Mice

C57BL/6 mice (6-8 week old female) were purchased from Jackson Laboratories and BL6-CD45.1 mice (6-8 week old female) were purchased from Charles River. All mouse procedures were approved by the Johns Hopkins University Institutional Animal Care and Use Committee and were compliant with the Guide for the Care and Use of Laboratory Animals (8th ed. The National Academic Press. 2011).

Antibodies

Therapeutic antibodies aCTLA-4 IgG1 (9D9), aCTLA-4 IgG2a (9D9), aPD-1 (4H2), anti-DT mIgG1 (1D12) and anti-DT mIgG2a (1D12) were acquired in collaboration with Alan Korman and Mark Selby at Bristol-Myers Squibb. Dosing per injection was 200 ug for all antibodies, administered IP in 200ul PBS.

Immunohistochemistry antibodies included CD3 (SP7), ThermoScientific; CD4 (1), SinoBiological; FoxP3(D608R), Cell Signaling.

Flow cytometry staining antibodies included CD4-Pacific orange (RM4-5) Invitrogen; CD4-FITC (GK1.5), CD8-PerCP/Cy5.5 (53-6.7), CD44-Pacific Blue (IM7), CD11b-AlexaFluor700 (M1/70), CD11c-FITC (N418), F4/80-Pe/Cy7 (BM8), CD16.2(FcRIV)-PE (9E9), FoxP3-APC (FJK-16s), CD25-PerCp/Cy5.5 (PC61), CTLA4-

PE (UC10-4B9), CD86-PE/Cy5 (GL-1), IFN-gamma-PE/Cy7 (XMG1.2), CD45-BV605 (30-F11), IFN γ -APC(XMG1.2), Gzb-Pacific Blue (GB11), BioLegend; GranzymeB-PE (16G6), CD4-PerCP Cy5.5 (RM4-5), Viability Dye- APC-Cy7, CD8-FITC (53-6.7), CD44-AF700 (IM7), TNF α -PE (MP6-XT22), eBioscience; TNF-APC (MP6-XT22), BD Biosciences; IL-2-PE-CF594 (JES6-5H4), BD Horizon.

LM/2a Tumor Outgrowth and Infiltration Studies

5×10^5 B16F10 cells were implanted between the skin and peritoneal cavity on day 0. On day 5, mice were vaccinated via the tail vein with Listeria or given sham treatment. On days 5, 7, and 9, mice were given 200ug (in 200ul PBS) of blockade antibodies or PBS alone. On day 18 mice were sacrificed. Tumor volume was calculated by the following equation: $(\text{Length} \times \text{Width}^2)/2$. Cell number of spleen and lymph node were counted on a hemocytometer while cell numbers of tumor infiltrate were acquired by flow cytometry. For Cytokine intracellular staining, animals sacrificed and tumors were harvested 10 days after implantation. Whole tumor suspension was incubated with PMA and Ionomycin for 4.5 hours. Cells were fixed for 30 minutes in Fixation/Permeabilization buffer by BD Bioscience (Cat. No. 554714 and 554715) before proceeding to stain.

Cytokine Array

Blood serum was collected by cheek bleed on days 8 and 11, then by incision of the IVC on day 14. Blood sat to clot for 10 minutes then was centrifuged and serum was harvested. The Luminex Biorad Mouse Group 1 23-plex assay (#M60-009RDPD) was conducted following vendor guidelines. Serum samples were diluted 1:4. Standard curves were generated and within the normal ranges expected with the exception of a reduced range for GMCSF. IL-4 was not detected.

Statistics:

Statistical significance for bar graphs was determined with a one-sided or two sided non-Paired students T test (*= $P < .05$, **= $P < .001$, ***= $P < .0001$). Statistical significance for Kaplan-Meier survival graphs was determined by Log-Rank Test.

Results

*Lymphocyte and Systemic Cytokine levels are increased by vaccination +
checkpoint blockade.*

We hypothesized that the enhanced tumor clearance due to combination therapy may be due to an enhanced effector T cell response. Thus, we sacrificed animals treated in the above strategy 10 days after tumor implantation, re-stimulated TIL *ex vivo* with PMA and Ionomycin, and analyzed the lymphocytes for their ability to produce effector cytokines. We found that after vaccination, Listeria and both aCTLA-4 antibodies enhance Granzyme B and Interferon Gamma production by TIL and reduce the number of cells that produce zero measurable cytokines. However, administration of aCTLA-4 (D) enhanced cytokine production and multi-functionality of TIL to a greater degree than both LM or aCTLA-4 (ND) monotherapies. The combination LM+aCTLA-4 (D) led to the greatest cytokine production, although it was not significantly higher than aCTLA-4 (D) alone (Figure 4-1a-b). To analyze the levels of systemic cytokines within mice, we performed blood cytokine analysis by acquiring blood serum from animals at 3,7, and 11 days after vaccination. 3 days after vaccination, systemic cytokine levels are generally elevated in mice that have received LM and enhanced further with the addition of checkpoint antibodies (Figure 4-2). Interestingly, we noted an overall increase in all measured systemic cytokine levels in untreated animals as well as most measured systemic cytokine levels in treated animals over time. On day 7 and 11, differences between treated and untreated groups became less clear (data not shown).

Combination LM-M+aCTLA4-IgG2a therapy robustly depletes Tregs in the tumor and allows for Tumor infiltration.

Because we observed increases in functionality of tumor immune infiltrate, we then analyzed the abundance of Treg and Teff lymphocytic infiltrate in the tumor microenvironment and periphery. We firstly examined the expression of CTLA-4 across cell types and confirmed that tumor infiltrating Treg highly express CTLA-4, even when compared to their peripheral counterparts (Figure 4-3a). We then analyzed mice treated as in Figure 3-1a for peripheral and Tumor infiltrating CD4⁺ FoxP3⁺ Treg. Not surprisingly, while Treg in the periphery stay relatively constant (data not shown) independent of treatment, Tumor infiltrating Treg percentages are highly reduced in LM treated, as well as aCTLA-4 (D) treated animals. When LM+aCTLA-4 (D) combination strategy is applied, Treg generally account for only 1-5% of CD4⁺ cells in the tumor as opposed to ~40% in untreated animals (Figure 4-3b-c). We next analyzed the number of Infiltrating lymphocytes in each of our treatments and show infiltration of lymphocyte very closely follows the depression of Treg percentages. LM increases infiltrate of both CD4⁺ and CD8⁺ cells as a monotherapy. However, aCTLA-4 (D) as a monotherapy or in combination with LM strongly induces infiltration of lymphocytes into the tumor environment (Figure 4b). Interestingly, almost all lymphocytes in the tumor are CD44⁺ in the untreated group, and this number generally does not increase with most treatments (data not shown). Because the CD4⁺ and CD8⁺ Tumor infiltrate increases concurrently with the decrease in Tregulatory cells, this treatment strategy allows for a high Teff:Treg ratio. Lastly, we stained for the presence of CD3 positive infiltrating cells across our

treatment groups using immunohistochemistry (IHC) on FFPE tumors (Figure 4-4a). While LM treatment alone shows a moderate increase in infiltrating CD3+ cells (red), aCTLA-4 (D) alone or in combination with LM vastly increases the lymphocytic infiltrate in the tumor. In fact, we observe foci of CD3+ cells in the middle of tumor areas that no longer express the pigment melanin.

Figure 4-1

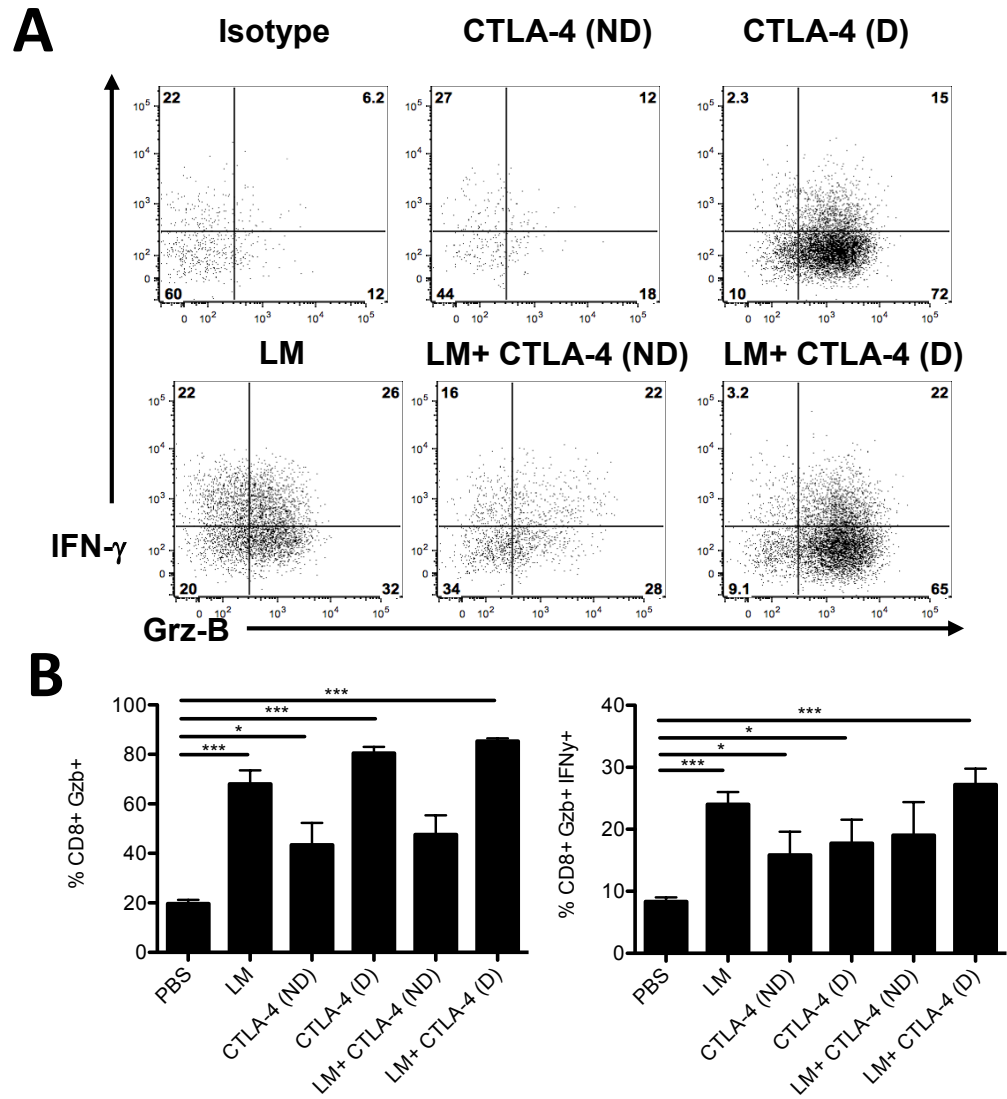


Figure 4-1: Lymphocyte and systemic cytokine levels are increased by vaccination + checkpoint blockade. **(A)** Mice were implanted with tumor and treated as in Figure 3-1. On Day 18, TIL were harvested and restimulated with PMA+Ionomycin and cytokine expression was examined by FACS. **(B)** Graph of Data in (A).

Figure 4-2

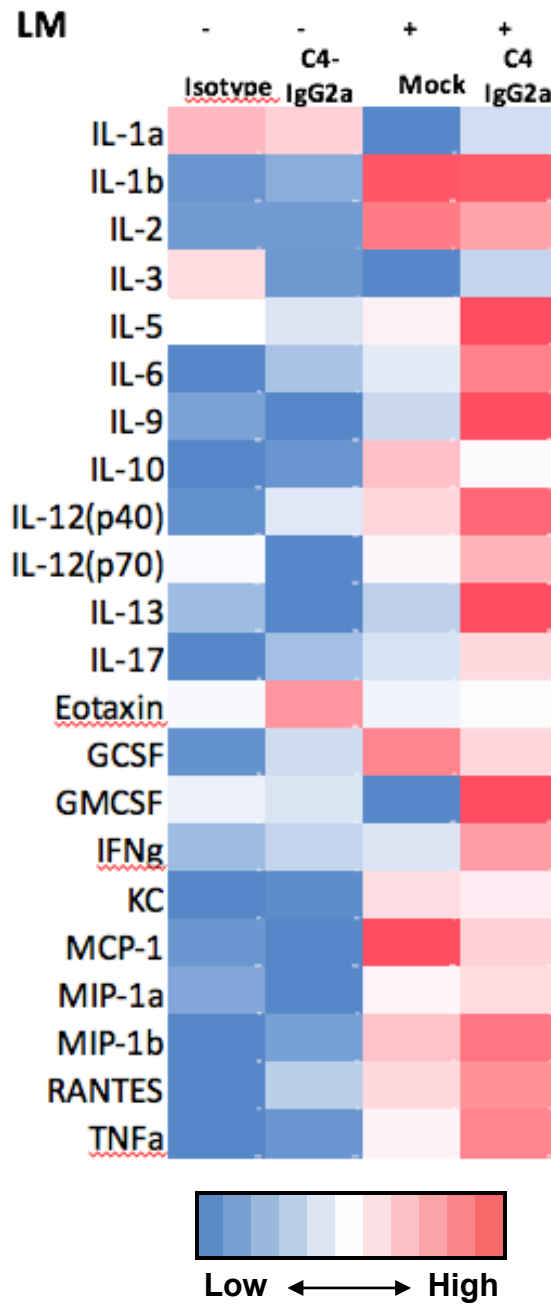


Figure 4-2. LM vaccination increases peripheral cytokines: 8 days after treatment, animals were bled via the tail vein and serum was collected. Serum was

diluted 1:4 and applied to a Luminex array and cytokines were measured. Data is normalized in a heat map within cytokine groups.

Figure 4-3

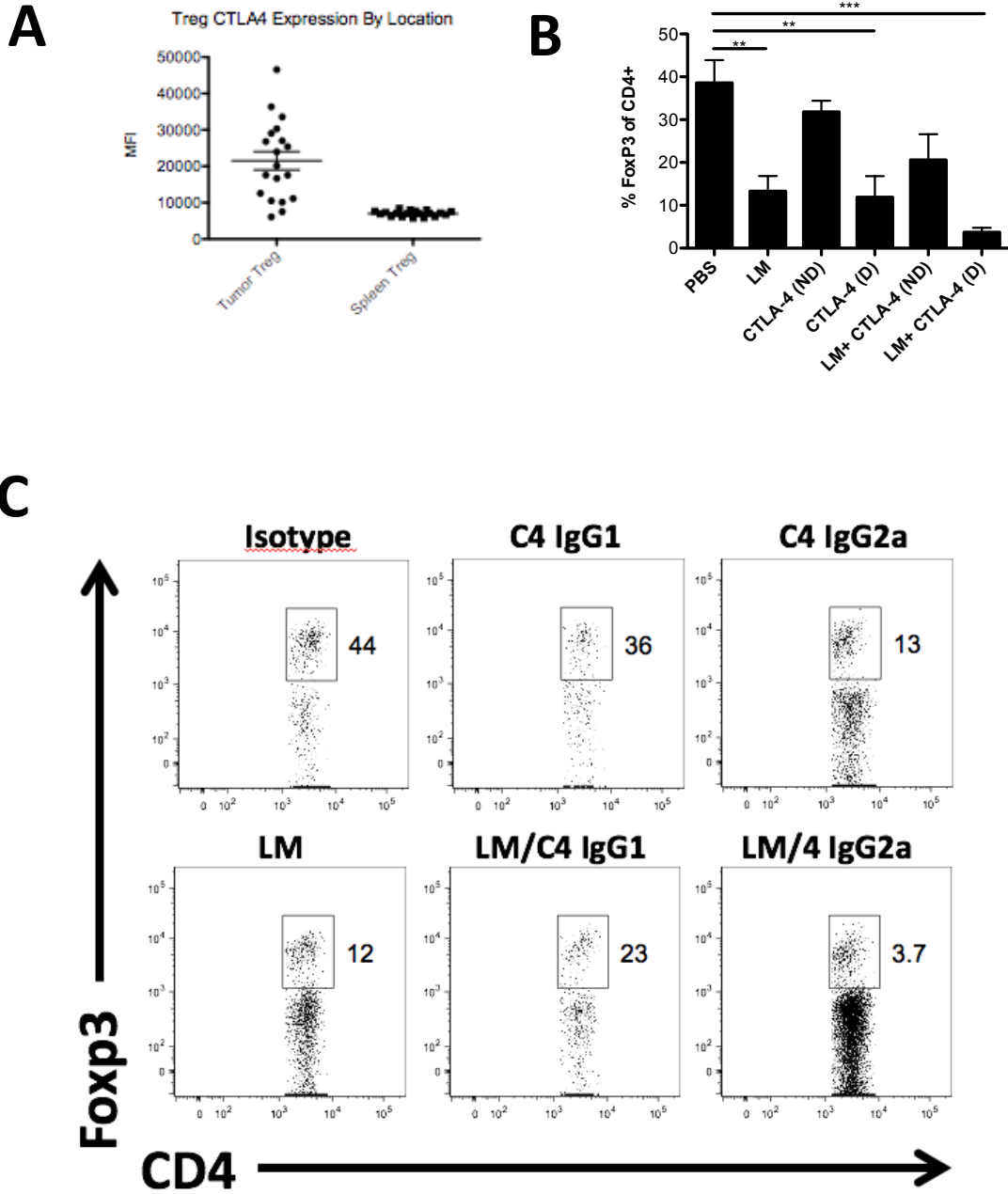
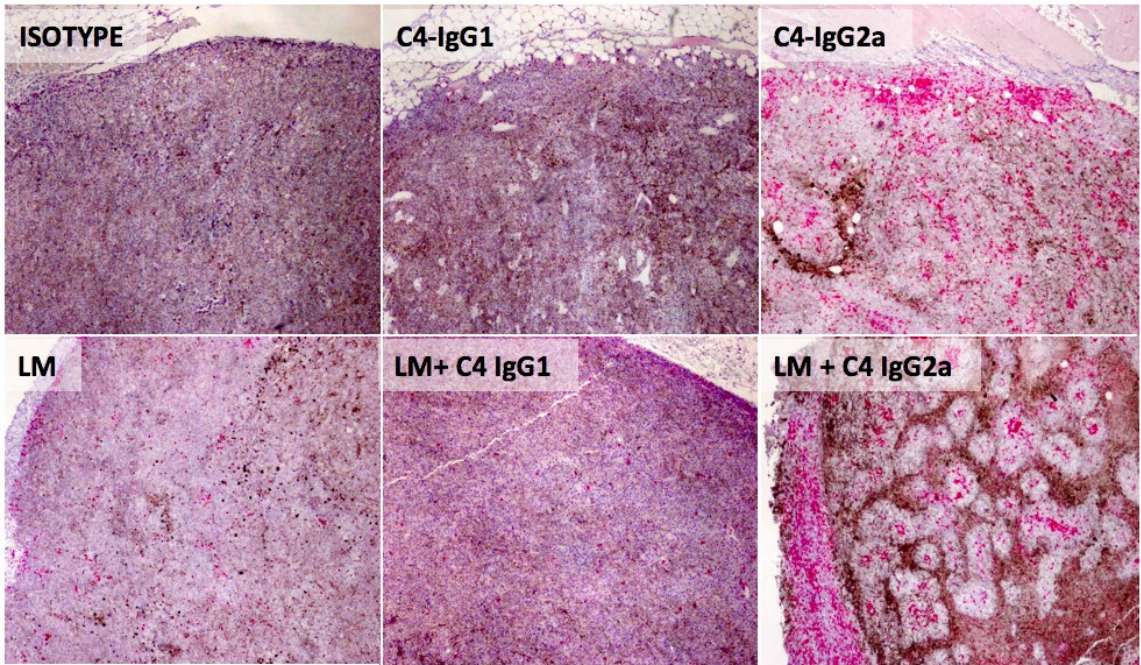


Figure 4-3: *Tregulatory cells are effectively depleted with LM and aCTLA-4 (D) strategies.* (All plots represent data collected on day 18 after treatment as in Figure 1a. **(A)** CTLA4 MFI on FoxP3+ cells across all treatment groups as measured by flow cytometry. All treatment groups were binned together and expression was examined based on location of cells. **(B-C)** Flow Cytometry plots tumor infiltrating CD4+FoxP3+. Cells were gated on FSC/SSC and vitality dye negative populations.

Figure 4-4

A



B

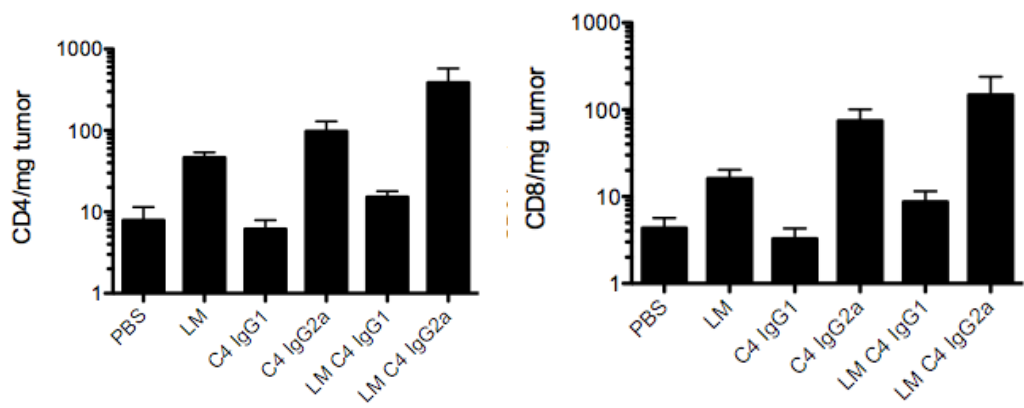


Figure 4-4: Effector cell infiltrate is greatly increased with LM+aCTLA-4 vaccination. **(A)** IHC of FFPE stained tumor sections, CD3+ cells in red. Bar graphs and FACS plots are representative of multiple similar experiments with 5 mice per group. IHC was performed in two separate experiments on a total of 5 or more mice. **(B)** Absolute numbers of tumor infiltrating CD4 and CD8 cells were analyzed by flow cytometry and divided by wet weights of tumors to determine cell number and cell number per mg tumor. Teff/Treg ratio was defined as $\#CD4+FoxP3-/\#CD4+FoxP3+$.

CHAPTER V

Fc Gamma receptors are indispensable for the anti tumor effects of CTLA4 IGG2a

Introduction

Antibody dependent cellular cytotoxicity (ADCC) is the phenomenon by which antibodies aid in the killing of cells. Antibodies are comprised of several different structural and functional components. For the sake of this introduction, we will focus on the Fab portion and the Fc portion. Endogenous or artificially introduced antibodies bind to their target cells at the variable region, or Fab, of the antibody, which is exquisitely specific for the target. The other portion of the antibody structure is the constant region, or Fc. The Fc portion of the antibody is the ligand for Fc-Receptors, which are Fc-binding proteins located on phagocytic or cytotoxic cells throughout the body. While multiple cell types can express Fc receptors, natural killer (NK) cells and macrophages express the widest variety in the highest abundance, and thus are thought to be the main cellular mediators of ADCC.

There are several classes of Fc Receptors, each with specific functions. Generally grouped into activating Fc receptors, which stimulate the cell bearing them and induce apoptosis of the antibody-bound target, and inhibitory Fc receptors, which do not aid in ADCC and are thought to prevent phagocytosis or killing of the target. Recently, isotypic differences in checkpoint blockade antibodies have been implicated in the efficiency of ADCC based depletion¹⁰⁰. In mice, isotype IgG2a binds Fc receptors with higher affinity, and thus corresponds with highly effective depletion while IgG1 is less effective at binding Fc receptors and thus mediating ADCC¹⁰¹.

Chapter Specific Materials and Methods

Cell Lines

B16F10 and CT26 were acquired from ATCC (CRL-6475, and CRL-2639 Respectively) and were cultured in Complete RPMI (10%FBS, 100u/ml penicillin, 100ug/ml streptomycin, 250ng/ml amphotericin, 1mM sodium pyruvate, NEAA).

Mice

C57BL/6 mice (6-8 week old female) were purchased from Jackson Laboratories and BL6-CD45.1 mice (6-8 week old female) were purchased from Charles River. FoxP3 DTR mice were a gift from Dr. Drew Pardoll and FcγR^{-/-} (B6.129P2-FcγR1^{tm1RavN12}) breeder mice were purchased from Taconic and bred in Johns Hopkins Facilities. All mouse procedures were approved by the Johns Hopkins University Institutional Animal Care and Use Committee and were compliant with the Guide for the Care and Use of Laboratory Animals (8th ed. The National Academic Press. 2011).

Antibodies

Therapeutic antibodies aCTLA-4 IgG1 (9D9), aCTLA-4 IgG2a (9D9), aPD-1 (4H2), anti-DT mIgG1 (1D12) and anti-DT mIgG2a (1D12) were acquired in collaboration with Alan Korman and Mark Selby at Bristol-Myers Squibb. Dosing per injection was 200 ug for all antibodies, administered IP in 200ul PBS.

Flow cytometry staining antibodies included CD4-Pacific orange (RM4-5) Invitrogen; CD4-FITC (GK1.5), CD8-PerCP/Cy5.5 (53-6.7), CD44-Pacific Blue (IM7), CD11b-AlexaFluor700 (M1/70), CD11c-FITC (N418), F4/80-Pe/Cy7 (BM8), CD16.2(FcRIV)-PE (9E9), FoxP3-APC (FJK-16s), CD25-PerCp/Cy5.5 (PC61), CTLA4-

PE (UC10-4B9), CD86-PE/Cy5 (GL-1), IFN-gamma-PE/Cy7 (XMG1.2), CD45-BV605 (30-F11), IFN γ -APC(XMG1.2), Gzb-Pacific Blue (GB11), BioLegend; GranzymeB-PE (16G6), CD4-PerCP Cy5.5 (RM4-5), Viability Dye- APC-Cy7, CD8-FITC (53-6.7), CD44-AF700 (IM7), TNF α -PE (MP6-XT22), eBioscience; TNF-APC (MP6-XT22), BD Biosciences; IL-2-PE-CF594 (JES6-5H4), BD Horizon.

LM/2a Tumor Outgrowth and Infiltration Studies

5×10^5 B16F10 cells were implanted between the skin and peritoneal cavity on day 0. On day 5, mice were vaccinated via the tail vein with Listeria or given sham treatment. On days 5, 7, and 9, mice were given 200ug (in 200ul PBS) of blockade antibodies or PBS alone. On day 18 mice were sacrificed. Tumor volume was calculated by the following equation: $(\text{Length} \times \text{Width}^2)/2$. Cell number of spleen and lymph node were counted on a hemocytometer while cell numbers of tumor infiltrate were acquired by flow cytometry. For Cytokine intracellular staining, animals sacrificed and tumors were harvested 10 days after implantation. Whole tumor suspension was incubated with PMA and Ionomycin for 4.5 hours. Cells were fixed for 30 minutes in Fixation/Permeabilization buffer by BD Bioscience (Cat. No. 554714 and 554715) before proceeding to stain.

Statistics:

Statistical significance for bar graphs was determined with a one-sided or two sided non-Paired students T test (*= $P < .05$, **= $P < .001$, ***= $P < .0001$). Statistical significance for Kaplan-Meier survival graphs was determined by Log-Rank Test.

Results

LM-M/CTLA4 Combination therapy are FcR dependent

Previous research has shown that IgG2a dependent ADCC occurs through Fc gamma receptor 4 (FcγRIV). We hypothesized that LM may synergize with aCTLA4 and enhance ADCC through activation of macrophages to express higher levels of surface FcγRIV. To assess this we treated WT mice as in Figure 1a and measured FcγRIV expression by flow cytometry. Both LM (not significant) and aCTLA-4 (D) administration increased the number of FcγRIV + macrophages (Figure 5-1b) and the MFI of FcγRIV (Figure 5-1a). We next examined the outgrowth and lymphocytic compartment of Fc common gamma chain knockout mice (FcγR^{-/-}). Unsurprisingly, FcγR^{-/-} mice are unable to control tumor to the same degree as WT mice when administered aCTLA-4 (D) (Figure 5-2a). Tregulatory cells are still reduced with LM treatment in these animals, but not with aCTLA-4 (D) treatment, showing that Fc receptors are necessary for aCTLA-4 (D) dependent ADCC of Treg (Figure 5-2b). Concurrently, while LM+aCTLA4 (D) increases CD4⁺ and CD8⁺ TIL in WT animals, FcγR^{-/-} animals show a marked reduction in the ability to induce an immune infiltrate when treated with aCTLA-4 (D) alone (Figure 5-2c). Treatment LM increases these numbers, but cannot fully rescue infiltration in a WT vaccinated animal. All these data suggest that aCTLA-4 (D) reduces tumor Treg through Fc Gamma receptors, and that our vaccination strategy not only acts through the presence of these receptors, but can also induce and increase their expression.

Figure 5-1

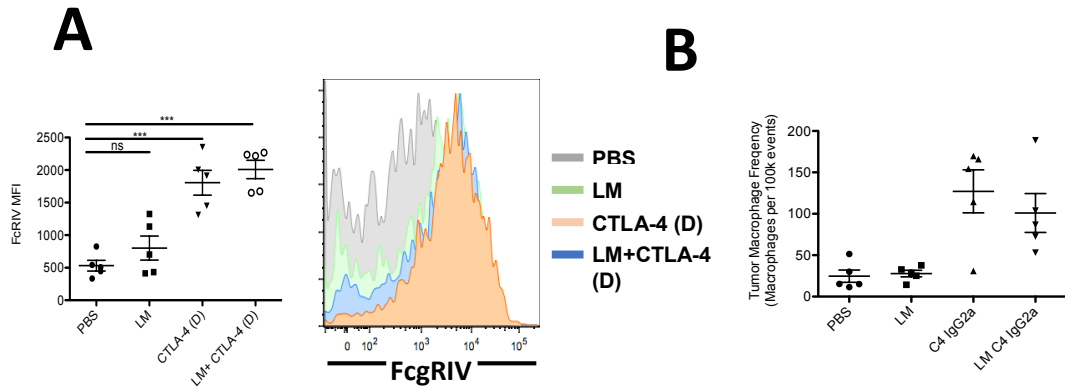


Figure 5-1: *CTLA4 (D)* therapeutic effect is ablated in *Fcgr*^{-/-} mice. Mice were treated according to Figure 3-1. **(A)** 10 Days after tumor implantation, tumors from WT animals were harvested and analyzed via flow cytometry for FcRIV expression on CD11b+F4/80+ cells. Graph of FcRIV MFI and representative histograms of FcRIV MFI in CD11b+F4/80+ Cells. **(B)** Macrophage frequency was measured by calculating the number of CD11b+F4/80+ Cells per 100,000 events. Data is representative of at least 2 similar experiments with 5 mice per experiment.

Figure 5-2

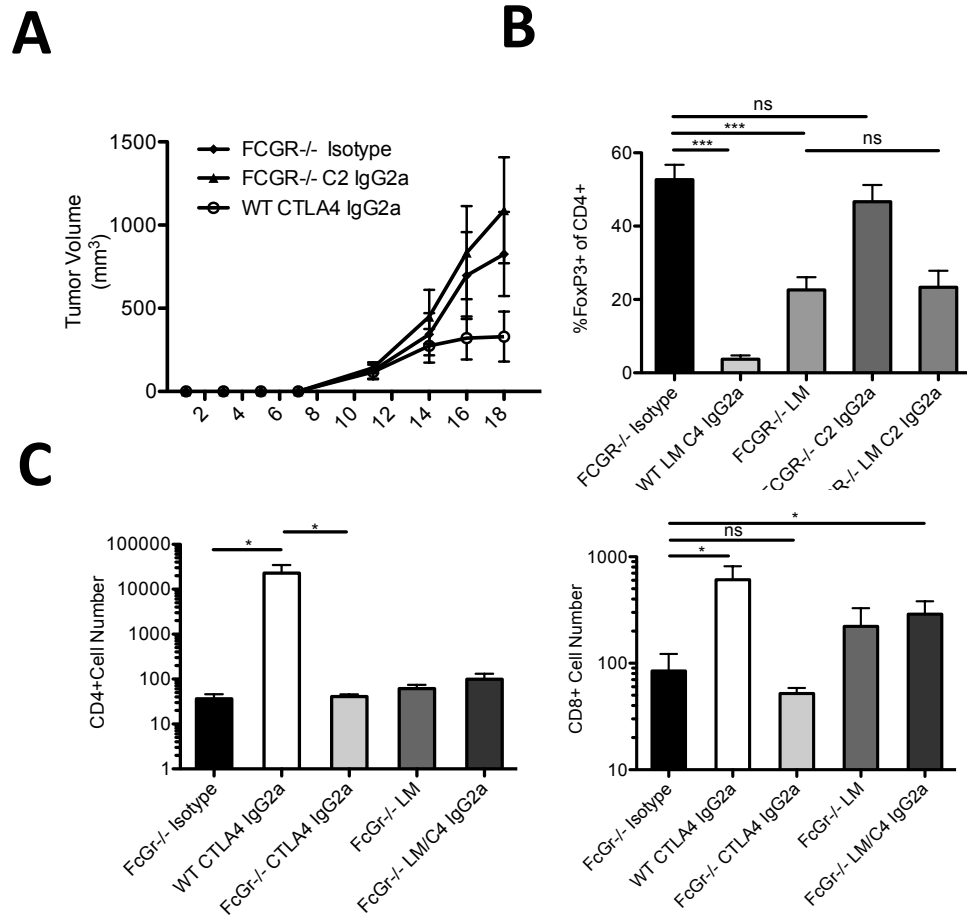


Figure 5-2. Outgrowth and Treg Depletion by CTLA-4 are Fc receptor dependent. (A) WT or FcGr^{-/-} mice, treated as in Figure 3-1, were measured and followed for outgrowth. (B,C) 18 Days after tumor implantation, WT or FcGr^{-/-} TIL was analyzed by Flow cytometry. Cell numbers and frequencies were calculated as in Figure 3. Data is representative of at least 2 similar experiments with 5 mice per experiment.

CHAPTER VI

**Therapeutic Intratumoral Injection of CDN leads to acute rejection of B16F10
Through modulation of the Tumor Microenvironment**

Introduction

Recent data suggests that the cGAS-STING axis not only determines outcomes to bacterial and viral insult, but also to self-DNA in cancer models^{96,102-108}. STING deficient mice lack the ability to reject highly immunogenic tumors, and have accelerated tumor outgrowth in less immunogenic tumor models. Interestingly, these studies also show that tumor DNA can be found in dendritic cells, and that these cells are necessary to initiate an adaptive immune response¹⁰⁷. Sparked by these discoveries, studies have begun to utilize CDN as an immunotherapeutic agent. Administration of small doses of CDN intravenously (IV) can aid in initiating an adaptive immune response, however, IV dosing of this agent seems to be delicate in that high concentrations of CDN can produce sub optimal or even immune suppressive conditions⁹⁵. If administered intratumorally (IT), some tumor cell lines are directly effected by sting activation and undergo apoptosis. However, this direct killing of tumor cells seems to be a rare event, IT CDN administration more often induces tumor regression by inducing cellular infiltrate and inflammatory cytokine environment¹⁰².

While the effects of sting signaling on adaptive immune cells have begun to become elucidated, relatively little data has been shown on the effects of CDN on the stromal cell compartment. Endothelial cells have been shown to produce interferon- β after CDN administration¹⁰⁹, but no study has shown the importance of TNF α production on the tumor microenvironment, and no study has definitively shown that production of innate cytokines is necessary for acute tumor necrosis and immune infiltrate modulation. Additionally, we are the only group to use bone marrow chimeras to show the

dependence of tumor necrosis on STING sensing within stromal cells and that stromal cells play an indispensable role in mediating acute clearance of tumors using IT CDN.

Chapter Specific Materials and Methods

Cell Lines

B16F10 and CT26 were acquired from ATCC (CRL-6475, and CRL-2639 Respectively) and were cultured in Complete RPMI (10%FBS, 100u/ml penicillin, 100ug/ml streptomycin, 250ng/ml amphotericin, 1mM sodium pyruvate, NEAA).

Mice

C57BL/6 mice (6-8 week old female) were purchased from Jackson Laboratories and BL6-CD45.1 mice (6-8 week old female) were purchased from Charles River. FoxP3 DTR mice were a gift from Dr. Drew Pardoll and FcγR^{-/-} (B6.129P2-FcγR^{tm1RavN12}) breeder mice were purchased from Taconic and bred in Johns Hopkins Facilities. cGAS^{-/-} animals were a gift from Skip Virgin. STING^{-/-} animals are the Golden Ticket strain, and were a gift from Young Kim. Rag2^{-/-} animals were a gift from Jonathan Powell. IFNar^{-/-} (B6.129S2-Ifnar1^{tm1Agt/Mmjax}), TNFa^{-/-} (B6.129S-Tnftm1Gkl/J), and IL-6^{-/-} (B6;129S2-Il6^{tm1Kopf/J}) breeder pairs were purchased from Jackson laboratories and bred in Johns Hopkins Facilities. All mouse procedures were approved by the Johns Hopkins University Institutional Animal Care and Use Committee and were compliant with the Guide for the Care and Use of Laboratory Animals (8th ed. The National Academic Press. 2011).

Antibodies

For CDN studies antibodies used included CD11b-AF700 (M1/70), CD44-Pacific Blue (IM7), CD11c-FITC (N418), CD86-PE (GL-1), CD19 PerCP-Cy5.5 (6D5), Ly6C-BV605(HK1.4), CD45.2- APC (104), IA/IE- PerCP-Cy5.5 (M5/114.15.2), Ly6G- BV421

(1A8), CD16/32-BV510 (93), F4/80-PE-Cy7 (BM8), CD206-BV711 (C068C2), Ly6c-PerCP- Cy5.5 (HK1.4), and CD4- BV605 (GK1.5), Biolegend; NOS2-APC (CXNFT), NK1.1-PE (PK136), and CD8-PE-Cy7 (53-6.7), EBioscience; CD4-Pacific Orange (RM4-5), Life Technologies; CD45.1-FITC (A20) BD Pharmingen.

CDN Tumor Outgrowth and Infiltration studies

5×10^5 B16F10 cells were implanted between the skin and peritoneal cavity on day 0. Tumors were monitored until the group average was $\sim 80 \text{mm}^3$ and then treated with 100ug injections of CDN in 40ul PBS or PBS alone every other day for a total of three treatments. For chimera studies, a surplus of mice were implanted tumor, then when tumors were palpable, animals were selected and groups normalized to $\sim 80 \text{mm}^3$. Tumor outgrowth volume was measured by the equation $V = 1/2(\text{width}^2 * \text{length})$. 24 hours after treatment, some mice were sacrificed for tumor infiltrate studies by flow cytometry or for tumor lysate. Tumor lysate was made by resecting tumors and dissociating in Cell Lytic M (Sigma Cat no. C2978) with Protease Inhibitor Cocktail (Sigma S8820).

Elisa:

Elisas were purchased as kits as follows: Mouse IL-1b/IL-1f2 (Catalog No. MLB00c), Mouse GM-CSF (Catalog No. MGM00), Mouse IL-6 (Catalog No. M6000B), Mouse TNF-a (Catalog No MTA00B) R&D; VeriKine Mouse IFN γ Elisa (Catalog No 42400-2) PBL Assay Science; Mouse Inflammatory Cytokines Multi-analyte ELISArray Kit (MEM004a), Quiagen.

Statistics:

Results

Therapeutic Intratumoral Injection of CDN leads to acute rejection of B16F10.

Because CDN's have been shown to be potent adjuvants and because direct injection of adjuvant is now being used in clinical trials, we sought to understand the effect of adjuvant injection on the tumor microenvironment. To do this, we implanted B16F10 tumors in the flank of mice and treated mice with tumors of volume 80-100 cm³ with 3x 40 ul injections of 100ug RR-di adenosine CDN (Figure 6-1a). Within 48 hours of the first injection, redness and necrosis forms around the injection site. Within 5 days of injection, an eschar has formed and tumor is no longer palpable. At 8 days after first treatment, untreated animals have large tumors and may need to be sacrificed, but treated animals generally have only a eschars (Figure 6-1c,d). Occasionally injection and necrosis of the tumor is incomplete and healthy growing tumor can be seen, even around the site of injection (Figure 6-1e). Several weeks after injection, mice that have completely cleared tumor have healed but show reaction site vitiligo indicating the presence of an ongoing, melanin specific adaptive immune response (Figure 6-1f).

IT CDN injection causes a distinct cytokine and cellular profile in the tumor.

To gain an understanding into the cause of necrosis within the tumor, we performed extensive analysis of the systemic and tumor infiltrating cytokines and immune cells before and after intratumoral CDN administration. 24 hours after the initial injection, we sacrificed animals and analyzed spleen, tumor draining lymph node and tumor for cellular infiltrate via flow cytometry. Due to the acute nature of tumor rejection, we did not expect that adaptive immune infiltrate and killing would be enhanced in the tumor, and in fact injection of high dose CDN caused a decrease in T and

B cell numbers acutely (figure 6-2). This decrease in the lymphocytic compartment may be due to toxicity of high dose CDN to lymphocytic cells (unpublished data). On the contrary, CDN administration increased the number of tumor infiltrating CD11b+F4/80+ macrophages as well as CD11b+F4/80- neutrophils (these cells are further characterized by the high expression of Ly6g and low expression of Ly6c). NK cell numbers were not effected in the tumor. Interestingly, the tumor draining lymph node experiences a similar decrease in T cell percentages, though not B cell percentages, along with a large increase of high FSC and SSC cells that are a large percentage macrophages and other APC (Figure 6-3).

We next examined intratumoral cytokine levels by resecting tumors and creating whole tumor lysate. After tumors were homogenized and lysed, we performed a multiKine ELISA. 24 hours after the initial injection of CDN, we observed highly significant increases in the amount of IL-6, TNFa, IFNb, IL-1, and GMCSF within the tumor (Figure 6-4).

Figure 6-1

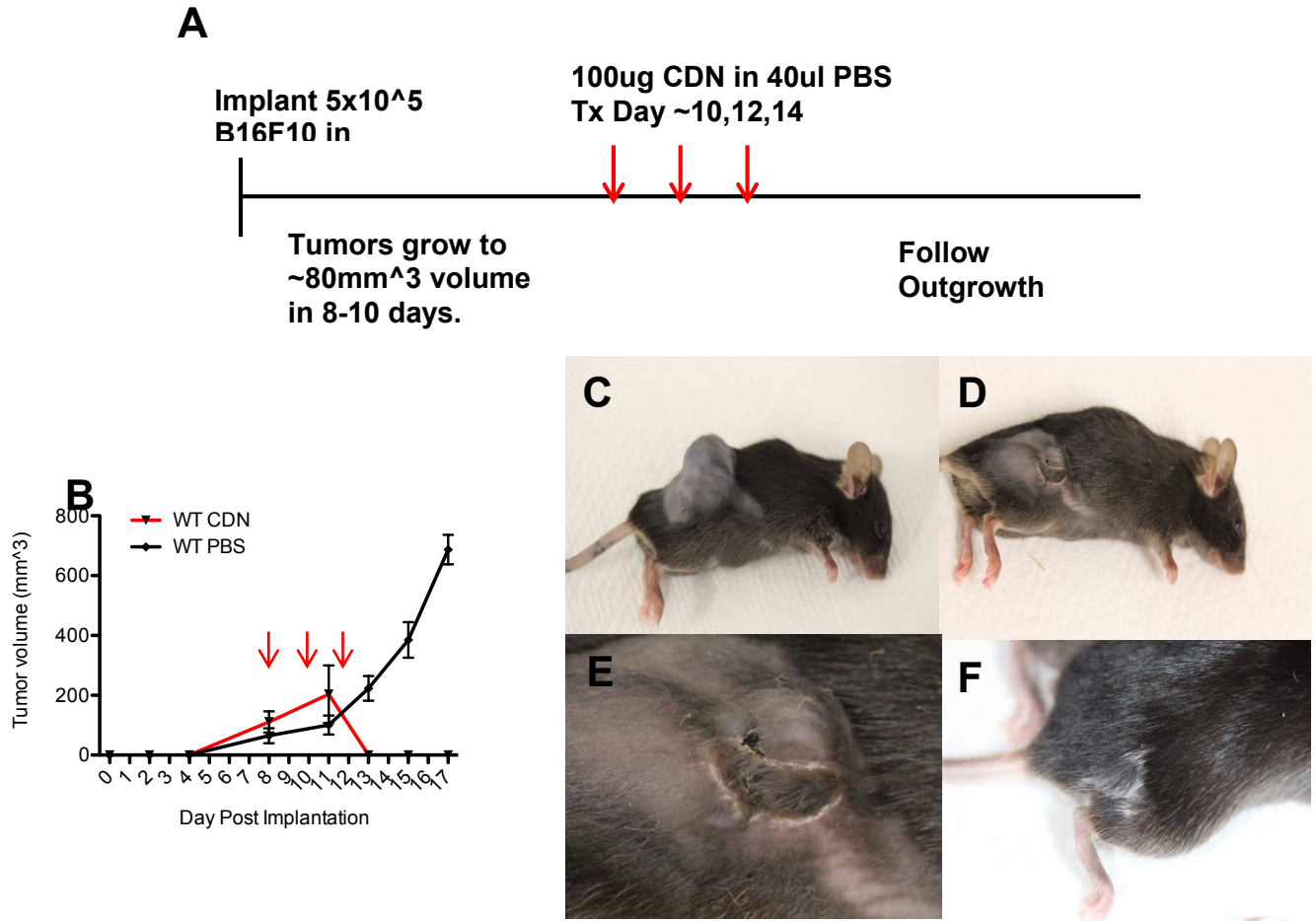


Figure 6-1: IT CDN treatment leads to tumor regression in B16F10 tumor bearing animals. (A) Animal treatment scheme. 5×10^5 B16F10 cells were implanted between the skin and peritoneal cavity on day 0. Tumors were monitored until the group average was $\sim 80 \text{mm}^3$ and then treated with 100ug injections of CDN in 40ul PBS or PBS alone every other day for a total of three treatments. (B) Outgrowth of animals treated as in (A). (C-D) Photos of tumors 8 Days after CDN (C) or PBS (D) show necrosis at the tumor site. (E) Close-up of necrosis in (D). (F) 3+ Weeks after CDN injection, mice show signs of vitiligo.

Figure 6-2

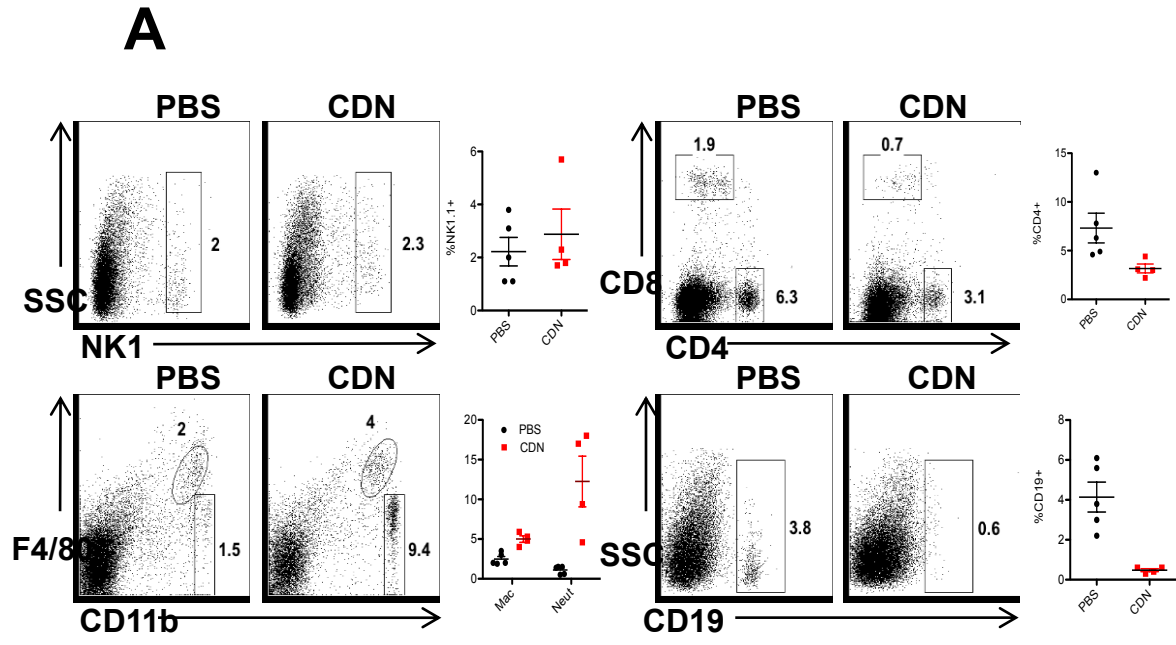


Figure 6-2: IT CDN changes tumor immune infiltrate. (A) 24 hours after IT CDN administration, mice are sacked and TIL was analyzed by flow cytometry.

Figure 6-3

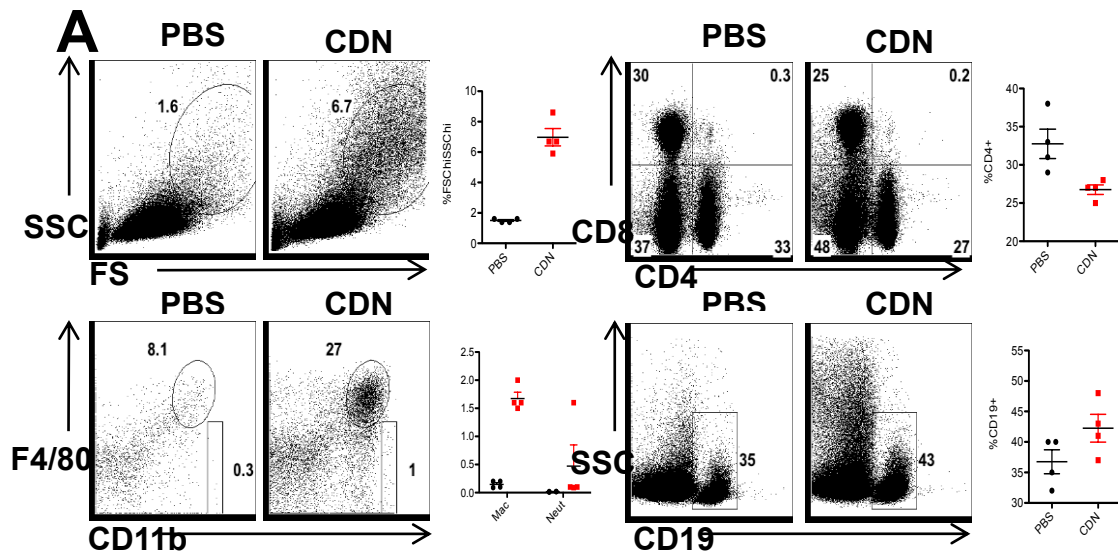


Figure 6-3: IT CDN changes tumor draining lymph node immune infiltrate. (A)

24 hours after IT CDN administration, mice are sacrificed and the tumor draining lymph node was analyzed by flow cytometry.

Figure 6-4

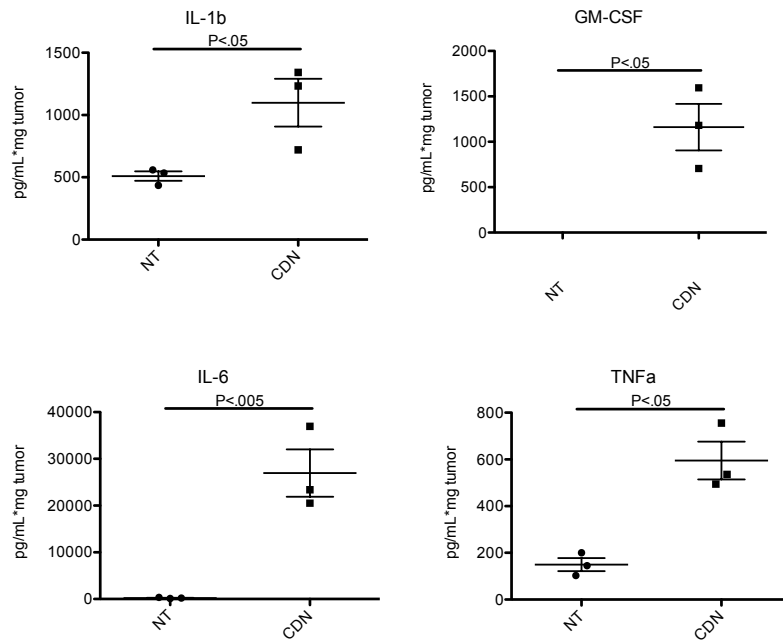


Figure 6-4: Cytokine concentrations in tumor microenvironment increase after IT CDN. 24 hours after IT CDN administration, tumor lysates were prepared as described in the above methods, and cytokine levels were measured by ELISA.

CHAPTER VII

TNF α production is necessary for IT CDN related necrosis and is produced by both stromal and bone marrow derived cells

Introduction

Previously, we have shown that the IT injection of CDN results in the increase of several cytokines and cell types within the TME. In looking more closely at the cytokine profile and cellular resulting from acute necrosis that we observe after, we hypothesized that a few key factors could be responsible for this necrosis. Most obviously, tumor necrosis factor has a well established function of inducing necrosis among various cell types expressing the receptor.

Tumor Necrosis Factor alpha (TNF α) is an inflammatory cytokine made of 3-17kD subunits in a trimeric form.¹¹⁰ It generally though of as a pro-inflammatory cytokine, it triggers dilation of blood vessels and leakage of fluid and cells into surrounding tissues. In systemic infection, massive release of TNF α can lead to septic shock.¹¹¹ In high doses, TNF α can also cause necrosis of tissues expressing the proper receptor. TNF α binds to one of two receptors, named TNFR-1 and TNFR-2. TNFR-1 is expressed by a wide variety of cell types, whereas TNFR-2 is generally only expressed on immune cells. Ligation of both receptors can lead to the transcription of NF κ B and pro-survival gene transcription through the binding of the TRADD scaffold protein. TNFR-1, however, is unique in it's ability to bind a Fas associated death domain (FADD) that can lead to cleavage and activation of pro-caspase 8 and pro-caspase 3. The activation of the effector caspase 3 in turn initiates apoptosis of the cell expressing TNFR-1.¹¹² Thus, TNF α plays an important roll in activating immune cells, but can have apoptic effects in non-immune cells.

TNF α is mainly produced by hematopoietic cells of the immune system.¹⁰² Macrophages in particular can produce large amounts of TNF α in response to ligation by TLR agonists. However it is now well characterized that TNF α is also produced by non-immune stromal cells such as endothelial cells, fibroblasts, and tumor cells.^{80,113,114}

Because a growing body of literature suggests the importance of cellular and cytokine infiltrate in tumor clearance, we sought to systematically eliminate possible contributors to this acute necrosis phenotype and observe the effect of the deletion.

Chapter Specific Materials and Methods

Cell Lines

B16F10 and CT26 were acquired from ATCC (CRL-6475, and CRL-2639 Respectively) and were cultured in Complete RPMI (10%FBS, 100u/ml penicillin, 100ug/ml streptomycin, 250ng/ml amphotericin, 1mM sodium pyruvate, NEAA).

Mice

C57BL/6 mice (6-8 week old female) were purchased from Jackson Laboratories and BL6-CD45.1 mice (6-8 week old female) were purchased from Charles River. FoxP3 DTR mice were a gift from Dr. Drew Pardoll and FcgR^{-/-} (B6.129P2-Fcgr1g^{tm1RavN12}) breeder mice were purchased from Taconic and bred in Johns Hopkins Facilities. cGAS^{-/-} animals were a gift from Skip Virgin. STING^{-/-} animals are the Golden Ticket strain, and were a gift from Young Kim. Rag2^{-/-} animals were a gift from Jonathan Powell. IFNar^{-/-} (B6.129S2-Ifnar1tm1Agt/Mmjax), TNFa^{-/-} (B6.129S-Tnftm1Gkl/J), and IL-6^{-/-} (B6;129S2-Il6tm1Kopf/J) breeder pairs were purchased from Jackson laboratories and bred in Johns Hopkins Facilities. All mouse procedures were approved by the Johns Hopkins University Institutional Animal Care and Use Committee and were compliant with the Guide for the Care and Use of Laboratory Animals (8th ed. The National Academic Press. 2011).

Chimeric animals were made by irradiating 6-12 week old animals with 2 doses of 6 gy separated by 3 hours. 3 hours after the second dose of irradiation, mice were reconstituted with 5-10 million cells of unirradiated donor bone marrow via tail vein injection and left to rest for at least 6 weeks. All chimeric animals were put on uniprim

feed at least 1 week before irradiation and removed from uniprim feed at least 1 week before tumor challenge.

CDN Tumor Outgrowth and Infiltration studies

5×10^5 B16F10 cells were implanted between the skin and peritoneal cavity on day 0. Tumors were monitored until the group average was $\sim 80 \text{mm}^3$ and then treated with 100ug injections of CDN in 40ul PBS or PBS alone every other day for a total of three treatments. For chimera studies, a surplus of mice were implanted tumor, then when tumors were palpable, animals were selected and groups normalized to $\sim 80 \text{mm}^3$. Tumor outgrowth volume was measured by the equation $V = 1/2(\text{width}^2 * \text{length})$. 24 hours after treatment, some mice were sacrificed for tumor infiltrate studies by flow cytometry or for tumor lysate. Tumor lysate was made by resecting tumors and dissociating in Cell Lytic M (Sigma Cat no. C2978) with Protease Inhibitor Cocktail (Sigma S8820).

Elisa:

Elisas were purchased as kits as follows: Mouse IL-1b/IL-1f2 (Catalog No. MLB00c), Mouse GM-CSF (Catalog No. MGM00), Mouse IL-6 (Catalog No. M6000B), Mouse TNF-a (Catalog No MTA00B) R&D; VeriKine Mouse IFN γ Elisa (Catalog No 42400-2) PBL Assay Science; Mouse Inflammatory Cytokines Multi-analyte ELISArray Kit (MEM004a), Quiagen.

Statistics:

Statistical significance for bar graphs was determined with a one-sided or two-sided non-Paired students T test (*= $P < .05$, **= $P < .001$, ***= $P < .0001$). Statistical significance for Kaplan-Meier survival graphs was determined by Log-Rank Test.

Results

TNF α Is required for Injection Site Necrosis

Because we observed distinct cellular and cytokine signatures after CDN injection, we hypothesized that these elements may be responsible for tumor site necrosis. To elucidate the minimal requirements for CDN-mediated injection site necrosis, we performed the same treatment scheme as in Figure 6-1a in a series of knockout mice. Unsurprisingly, while WT mice control tumors acutely, STING $^{-/-}$ animals lack the ability to sense CDN and clear tumor. cGAS $^{-/-}$ animals have no deficit in tumor clearance, showing that the upstream sensor of the sting pathway has no gross effect on the downstream signaling (Figure 7-1). RAG2 $^{-/-}$, IFN α $^{-/-}$, and IL-6 $^{-/-}$ animals all showed the same tumor site necrosis as WT animals. Interestingly, the type 1 Interferon receptor is a necessary mediator of many immune pathways, and thus tumors in these grow much faster (Figure 7-2a). This increased rate subverts some of the effect of CDN and CDN therapy is not curative in these animals in a B16 tumor system (Figure 7-2b). However, in a non-tumor bearing animal, injection site necrosis occurs in the same manner as a WT animal, showing that IFN α is not an important mediator of the acute response to CDN. Interestingly, the only animals to show absolutely no injection site necrosis after CDN injection were TNF α $^{-/-}$ animals.

Bone Marrow produced TNF α is predominates the tumor microenvironment.

We observed that TNF α is a necessary effector of CDN-mediated tumor site necrosis, and hypothesized that because bone marrow derived cells are largely responsible for the production of CDN, TNF α producing bone marrow cells would be required for injection site necrosis. To answer this, we developed a series of bone marrow

chimeras by irradiating WT or TNF α ^{-/-} hosts and reconstituting them with either WT or TNF α bone marrow. As hypothesized, animals with WT bone marrow have a more dramatic response to IT CDN therapy (Figure 7-3a). These animals have higher levels of intratumoral TNF α compared to their TNF α ^{-/-} bone marrow counterparts, clear tumor more efficiently than their counterparts, and have more injection site necrosis than their counterparts (Figure 7-3a-b). It should, however, be noted, that TNF α ^{-/-} \rightarrow WT bone marrow chimeric animals do form some necrosis and have a reduction in tumor burden when compared to TNF α ^{-/-} \rightarrow TNF α ^{-/-} chimeric controls. Based on these observations, we conclude that while both stromal and bone marrow derived TNF α contributes to necrosis, bone marrow derived TNF α dominates the milieu.

Figure 7-1

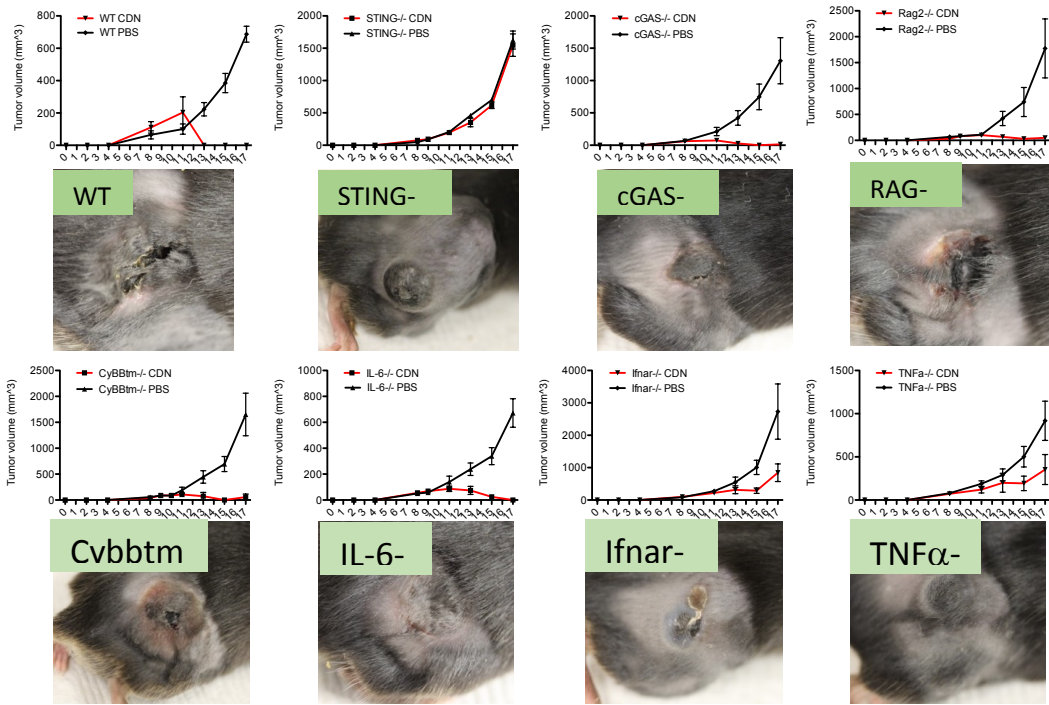


Figure 7-1: *TNFα* is required for injection site necrosis after IT CDN therapy. Tumors were implanted as above and outgrowth in knockout animals was assessed for volume and presence of necrosis.

Figure 7-2

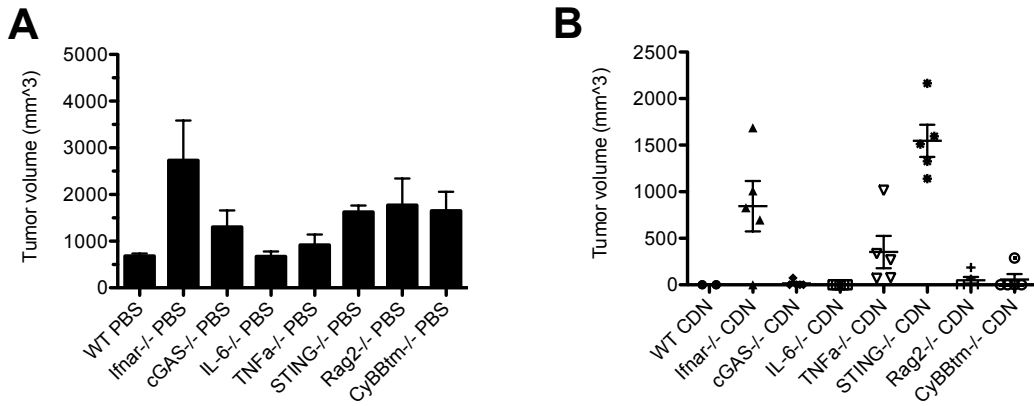


Figure 7-2: Tumor outgrowth is enhanced in *IFNar*, *STING*, *cGAS*, and *RAG*^{-/-} animals. (A-B) Tumor outgrowth on day 12 of untreated (A) and IT CDN treated (B) treated animals.

Figure 7-3

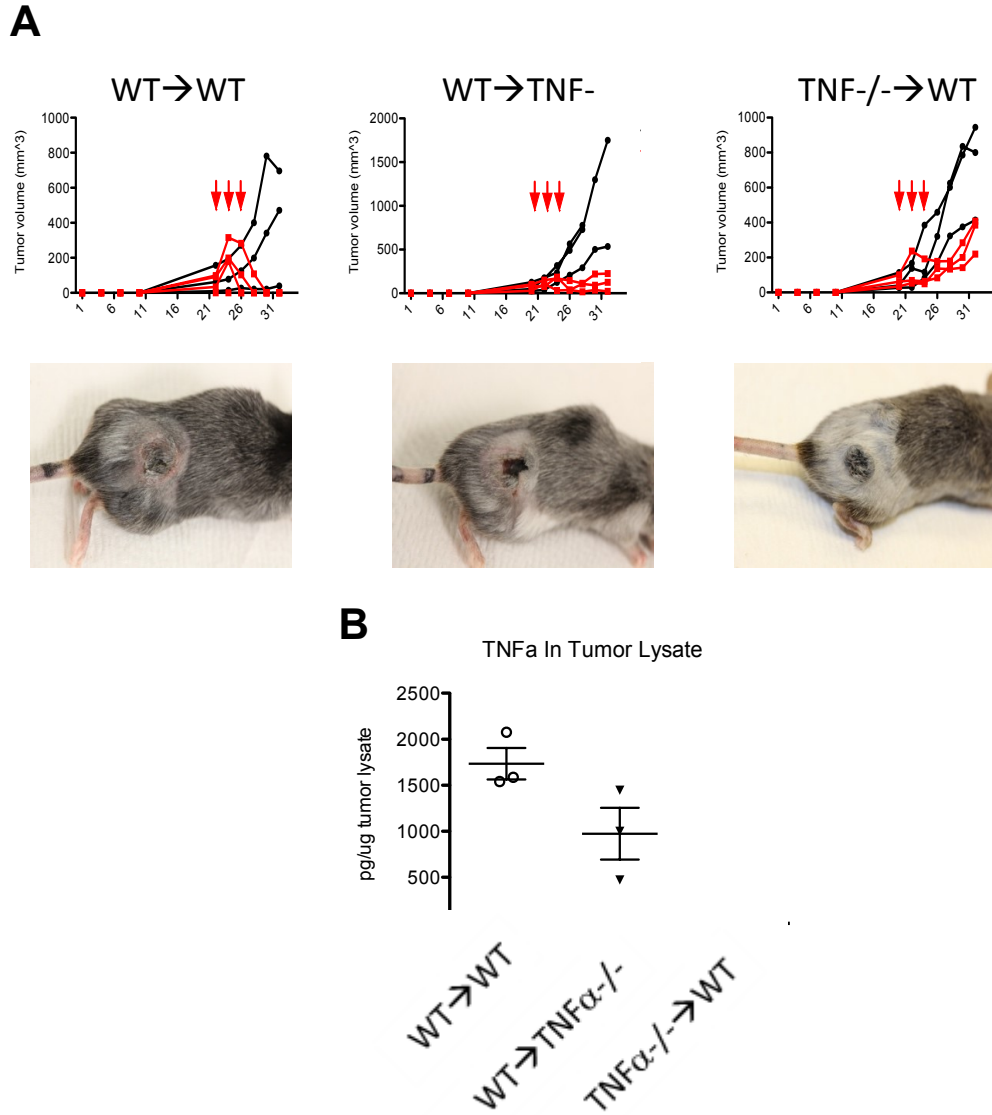


Figure 7-3: *TNFα* produced by both bone marrow and stroma aids in the clearance of *B16F10*. (A) Outgrowth plots and representative pictures of TNF/WT chimeric animals. (B) Elisa of tumor lysate taken 24 hours after IT CDN administration.

CHAPTER VIII

Both Bone marrow and stromal cell signaling are crucial for an IT CDN response

Introduction

With the exception of microglial cells, tissue resident macrophages, and few others, cells of the immune system are generally all derived from hematopoietic stem cells of bone marrow. The common lymphoid progenitor gives rise to all B cells, T cells, and NK cells, whereas the common myeloid progenitor gives rise to Basophils, neutrophils, and monocytes that spawn macrophages and dendritic cells. These cell subsets comprise the specialized cells of the immune system, and are exquisite at performing their duties within the immune system. However these are not, by a long stretch, the only cells that take part in immune reactions. Many cell types in the body have the capability to initiate an immune response through activation of any of several mechanisms, as discussed in the section “stromal cells” above. TLR agonists are not only found on immune cells, but on in the liver, on brain microglia, on epithelial cells in the gut, lung, and even musculature^{78,81}. Viral sensors like RIG-I and MDA5, which potently initiate production of type 1 interferons, can be found in many cell types including endothelial, epithelial, and fibroblast cells⁷⁹⁻⁸¹. Lastly, DNA sensors like cGAS as well as STING can be found in the cytosol and ER of multiple cell types¹¹⁵.

The prolific expression of these sensors means that, while far too often immunologist only consider the effects of adjuvants on immune cells, we should strongly consider the effect of these compounds on non-immune endothelial, epithelial, and other stromal cell subsets. Previous research has suggested that Type 1 interferon can be produced by CD31+ endothelial cells in response to IT CDN¹⁰⁹. While we have concluded that TNFa is vastly more important for acute necrosis in our system, we show

here, with a series of bone marrow chimeras, that sensing of CDN by stromal cells may be just as, or more important to generating acute inflammatory cytokines in the tumor microenvironment.

Chapter Specific Methods

Cell Lines

B16F10 and CT26 were acquired from ATCC (CRL-6475, and CRL-2639 Respectively) and were cultured in Complete RPMI (10%FBS, 100u/ml penicillin, 100ug/ml streptomycin, 250ng/ml amphotericin, 1mM sodium pyruvate, NEAA).

Mice

C57BL/6 mice (6-8 week old female) were purchased from Jackson Laboratories and BL6-CD45.1 mice (6-8 week old female) were purchased from Charles River. FoxP3 DTR mice were a gift from Dr. Drew Pardoll and FcγR^{-/-} (B6.129P2-Fcγ1^{tm1Rav}N12) breeder mice were purchased from Taconic and bred in Johns Hopkins Facilities. cGAS^{-/-} animals were a gift from Skip Virgin. STING^{-/-} animals are the Golden Ticket strain, and were a gift from Young Kim. Rag2^{-/-} animals were a gift from Jonathan Powell. IFNar^{-/-} (B6.129S2-Ifnar1^{tm1Agt}/Mmjax), TNFa^{-/-} (B6.129S-Tnfm1Gkl/J), and IL-6^{-/-} (B6;129S2-Il6^{tm1Kopf}/J) breeder pairs were purchased from Jackson laboratories and bred in Johns Hopkins Facilities. All mouse procedures were approved by the Johns Hopkins University Institutional Animal Care and Use Committee and were compliant with the Guide for the Care and Use of Laboratory Animals (8th ed. The National Academic Press. 2011).

Chimeric animals were made by irradiating 6-12 week old animals with 2 doses of 6gy separated by 3 hours. 3 hours after the second dose of irradiation, mice were reconstituted with 5-10 million cells of unirradiated donor bone marrow via tail vein injection and left to rest for at least 6 weeks. All chimeric animals were put on uniprim

feed at least 1 week before irradiation and removed from uniprim feed at least 1 week before tumor challenge.

Antibodies

For CDN studies antibodies used included CD11b-AF700 (M1/70), CD44-Pacific Blue (IM7), CD11c-FITC (N418), CD86-PE (GL-1), CD19 PerCP-Cy5.5 (6D5), Ly6C-BV605(HK1.4), CD45.2- APC (104), IA/IE- PerCP-Cy5.5 (M5/114.15.2), Ly6G- BV421 (1A8), CD16/32-BV510 (93), F4/80-PE-Cy7 (BM8), CD206-BV711 (C068C2), Ly6c-PerCP- Cy5.5 (HK1.4), and CD4- BV605 (GK1.5), Biolegend; NOS2-APC (CXNFT), NK1.1-PE (PK136), and CD8-PE-Cy7 (53-6.7), EBioscience; CD4-Pacific Orange (RM4-5), Life Technologies; CD45.1-FITC (A20) BD Pharmingen.

CDN Tumor Outgrowth and Infiltration studies

5×10^5 B16F10 cells were implanted between the skin and peritoneal cavity on day 0. Tumors were monitored until the group average was $\sim 80 \text{mm}^3$ and then treated with 100ug injections of CDN in 40ul PBS or PBS alone every other day for a total of three treatments. For chimera studies, a surplus of mice were implanted tumor, then when tumors were palpable, animals were selected and groups normalized to $\sim 80 \text{mm}^3$. Tumor outgrowth volume was measured by the equation $V = 1/2(\text{width}^2 * \text{length})$. 24 hours after treatment, some mice were sacrificed for tumor infiltrate studies by flow cytometry or for tumor lysate. Tumor lysate was made by resecting tumors and dissociating in Cell Lytic M (Sigma Cat no. C2978) with Protease Inhibitor Cocktail (Sigma S8820).

Elisa:

Elisas were purchased as kits as follows: Mouse IL-1b/IL-1f2 (Catalog No. MLB00c), Mouse GM-CSF (Catalog No. MGM00), Mouse IL-6 (Catalog No. M6000B), Mouse TNF-a (Catalog No MTA00B) R&D; VeriKine Mouse IFN γ Elisa (Catalog No 42400-2) PBL Assay Science; Mouse Inflammatory Cytokines Multi-analyte ELISArray Kit (MEM004a), Quiagen.

Statistics:

Statistical significance for bar graphs was determined with a one-sided or two sided non-Paired students T test (*= $P < .05$, **= $P < .001$, ***= $P < .0001$). Statistical significance for Kaplan-Meier survival graphs was determined by Log-Rank Test.

Results

Stromal STING sensing is required for injection site necrosis.

Because TNF α production by both bone marrow and stromal cells appeared to have an effect in the previous chimeric animals, we sought to understand the relative contributions of CDN sensing and STING signaling in bone marrow and stromal cells. Again, we made a series of bone marrow chimeras by irradiating WT or STING $^{-/-}$ hosts and reconstituting them with either WT or STING $^{-/-}$ bone marrow. After IT CDN therapy, only animals with STING competent (WT) bone marrow (GT \rightarrow WT, WT \rightarrow WT) became necrotic at the IT CDN injection site while chimeras devoid of stromal STING (WT \rightarrow GT, GT \rightarrow GT) had no such necrosis (Figure 8-1a). Similarly, only WT host animals have detectable TNF α , IFN β , IL-6, and GM-CSF in tumor lysate when measured by ELISA (Figure 8-1b). Interestingly, there is an effect of tumor regression in both sets of chimeric animals to a close degree, suggesting that while WT \rightarrow GT animals have no observable innate necrosis or cytokine response, there may be other mechanisms, like an ongoing adaptive response, that control the tumor to some degree.

To address the possibility of adaptive immune activation in all sets of chimeric animals, we analyzed the tumor draining lymph node(TDLN) infiltrate after CDN administration. All chimeras except GT \rightarrow GT experienced a significant infiltration of FSChi-SSChi cells into the TDLN (Figure 8-3). A large proportion of these cells were CD11b $^{+}$ CD11c $^{+}$ dendritic cells, and in all chimeras except GT \rightarrow GT these dendritic cells upregulated the activation co-stimulatory molecule CD86 after CDN administration. This suggests that DC can become activated directly or indirectly as a result of IT CDN administration.

Figure 8-1

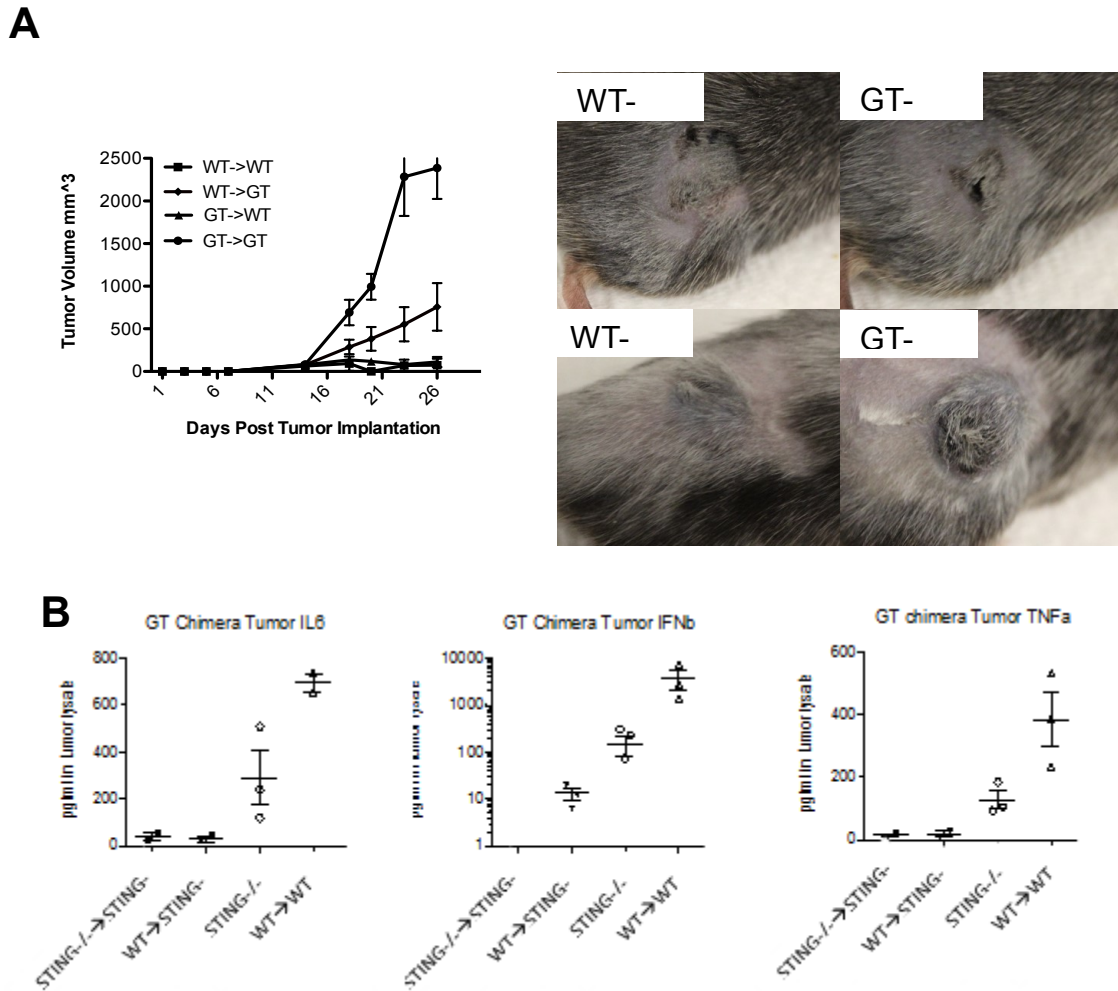


Figure 8-1: Tumor necrosis only occurs in mice with *STING* competent stromal cells. **(A)** Tumor outgrowth plots and pictures of chimeric animals treated with PBS or CDN. **(B)** ELISA of tumor lysate. 24 hours after IT CDN tumors were harvested and tumor lysate was made as described above.

Figure 8-2

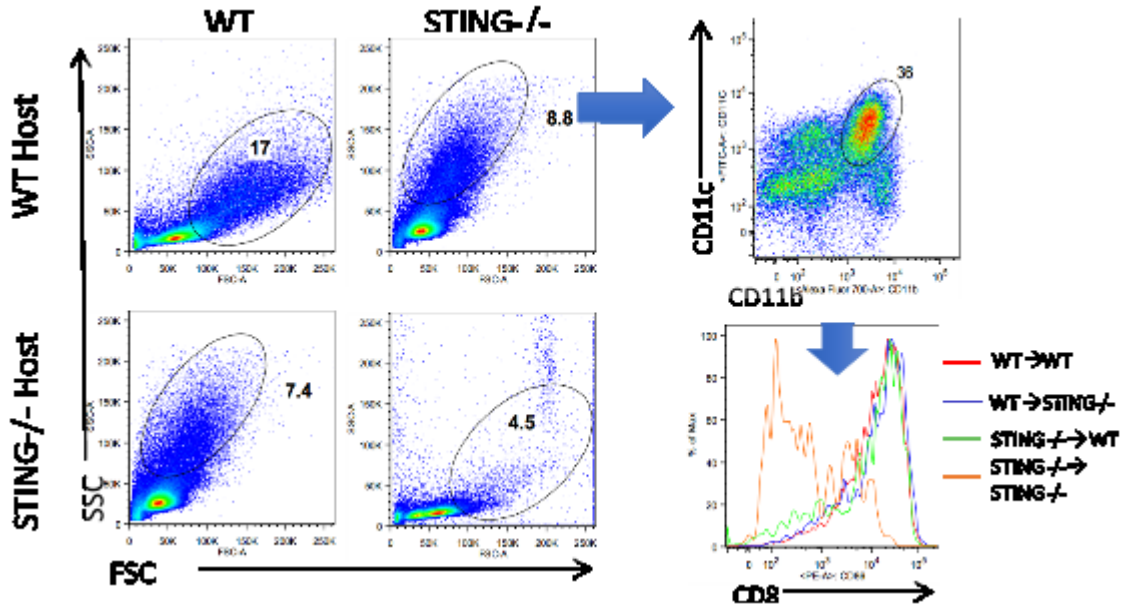


Figure 8-2: APC become activated via direct and indirect mechanisms after IT CDN. 24 hours after IT CDN administration, TDLN from CDN treated animals were harvested and analyzed by flow cytometry. APC were defined as high FSC/SSChi CD11c+CD11b+ cells. This population was then analyzed for CD86 expression by histogram.

CHAPTER IX

Conclusion and Discussion

Conclusion and Discussion

The tumor microenvironment presents many barriers and challenges to the immune system. However, these can be overcome through the use of agents to stimulate and shape the immune response as well as the tumor microenvironment in such a way that it becomes unaffected by these barriers. In the above work, we have used the current and growing wealth of knowledge about the immune system and about the tumor environment to design and apply therapies that have proven potent in causing the regression of aggressive lethal tumors. However, not only have we designed therapies, but we have used them to gain a more full understanding of the immune system as it pertains to cancer. We have elucidated previously undiscovered mechanisms pertaining to the development of T regulatory cells as well as the contribution of the tumor stroma to initiating an anti-tumor immune response. In the future, we aim to continue these studies and understand further details of the immune reaction to cancer.

Listeria+ Checkpoint Blockade Conclusions

Administration of immunotherapeutic agents has shown resounding success lately in clinical trials as well as pre-clinical models. However, along with the successes, clear limitations of these approaches have become apparent. Absence of tumor infiltrating lymphocytes in tumors corresponds with poor responses in patients, so increasing the tumor infiltrate and creating de-novo tumor responses is a crucial step to overcoming those hurdles. We report that vaccination with LM-MEL, an engineered listeria bacterium, reduces tumor burden, increases the number and percentage of multifunctional CD8⁺ Tumor infiltrating lymphocytes and reduces the percent of CD4⁺ lymphocytes that are FoxP3⁺ from ~40% to ~30%. The addition of aCTLA-4 (D) to this vaccine increases

tumor lymphocytic infiltrate over 10-fold and dramatically enhances tumor responses through further depletion of Tregulatory cells from ~30% to ~1%. This change in the cellular TIL compartment corresponds with a survival time of ~20 days when untreated to >40 days when treated.

The field of antibody engineering is becoming exquisitely attentive to Fc receptor binding. Antibodies that react with Tcells, such as PD-1, can be engineered to have absolutely no interaction with Fc receptors, while those that react with immunosuppressive compartments like Treg can be engineered to have maximal depletion efficiency. Unmentioned in these studies is manipulation of the other key element, the Fc receptor. Vaccines that can make depletion more efficient through upregulation of Fc receptors offer a double threat: activation of Tcells and enhancement of ADCC through monoclonal antibodies. To our knowledge, this is the first study that observes an increase in Fc expression as a result of vaccination. Listeria vaccination increases MFI of FcRIV by ~40%, and IgG2a increases this MFI another 2-4 fold. Our system is unfortunately not designed to determine if this upregulation of Fc receptor expression is functionally relevant, because LM, as we have shown, reduces Treg independently of Fc receptors and this confounds any conclusions we could draw.

It has been shown that checkpoint blockade reduces the fraction of Treg as a percent of total tumor infiltrate and that the resulting T_{eff}:Treg ratio is an important factor when predicting tumor clearance^{32,52}. While data concur completely in this regard the mechanism behind this observation is not fully addressed. It seems that while aCTLA-4 administration reduces the percent of FoxP3⁺ cells as a fraction of TIL, that

effect is mostly due to the induction of CD4⁺FoxP3⁻ infiltrate, not due to the obliteration of the Treg compartment. We in fact observe the opposite, a moderate increase in Treg in the tumor. aCTLA-4 has been shown to reduce surface activation markers and the suppressive capacity of Treg in in vitro suppression assays^{30,116}, but because we observe that tumor infiltration due to aCTLA-4 is isotype (IgG2a induces infiltrate while IgG1 does not) and Fc receptor dependent rather than Fab dependent, it seems unlikely that Treg dysfunction explains all of this phenotype. Similarly, because we observe that aCTLA-4 increases numbers of infiltrating macrophages and expression of Fc receptors on those macrophages, we hypothesize that there is another mechanism yet to be explored.

There are a few unexpected and unexplained results in our data. CD8 depletion does not lead to a complete abolition of tumor burden reduction. This is likely due to innate components of the immune system that we have left unexamined. Repolarization of TAM that might otherwise directly enhance tumor growth or activation of NK cells to kill tumor both may explain this vaccination effect. Additionally, aCTLA4 IgG1, supposedly “non-depleting” also leads to mild Treg depletion and increase of multifunctional CD8⁺ t cells. It should be noted that this antibody, while not optimized for depletion, still has the ability to bind Fc receptors, but with lower affinity. Lastly, the addition of LM-MEL to CTLA4 is mild, but consistent. In all our studies, this small combination effect always occurs.

IT CDN therapy Conclusions

We have shown here that IT CDN therapy has powerful effects leading to tumor clearance and long term survival of tumor bearing animals. In these studies, we have

focused on the innate acute effects of IT CDN therapy while also noting the long term adaptive effects that are initiated in the acute phase. Injection of high dose CDN leads to acute and often complete necrosis of the tumor area- an effect that is TNF α dependent. Our particular formulation of CDN, a mixed linkage RR-S2 cyclic di-adenosine, binds both mouse and human STING forms, though interestingly other CDN formulations we have worked with have higher potency at smaller doses in mouse models (unpublished data). Similarly, other formulations of CDN and sting agonists have shown differences in tumor clearance, induction of cytokines, and activation of an adaptive immune response.⁹⁶ However, we used only the human-binding CDN formulation because this is the product that will be taken forward into clinical trials. Additionally, other groups have assessed the use of lower dose CDN and through different vaccination routes to study the adaptive response, but that is also not what we focus on here.^{95,104} The efforts of these experiments focused on elucidating the importance and ability of the stromal cell compartment to add to effective tumor killing after CDN therapy.

We firstly showed efficacy and immune phenotype of tumors undergoing this therapy. The induction of multiple cytokines including IL-6, TNF α , IFN β , and GM-CSF was not surprising because we now understand that signaling downstream of STING stimulates both NF- κ B and IRF-3 activity. We showed that in the tumor, high dose CDN acutely deplete lymphocytic populations, which may necessitate the use of lower doses in humans. However, this does increase the infiltration of neutrophils and macrophages, cell subsets that we know can increase inflammation and produce TNF α . In the tumor draining lymph node, APC populations greatly increase and become activated,

as measured by the presence of CD86. Thus while this dose may not be optimal for resident lymphocytes, the potential exists to mount a robust adaptive immune response.

Importantly, we observe that acute CDN dependent tumor necrosis is not dependent on adaptive killing of the tumor, but rather TNF α necrosis alone. Using multiple genetic knockout mice, we show that RAG2, IL-6, cGAS, and IFN α are not responsible for tumor necrosis. However, STING $^{-/-}$ and TNF α $^{-/-}$ animals fail to show any injection site necrosis after IT CDN administration.

Using a series of bone marrow chimeras, we show that CDN dependent necrosis occurs only when host stromal cells are STING competent, and that TNF α can only be found in the TME when stromal cells are STING competent. Interestingly, none of our results have come in a binary fashion. It has become abundantly clear that the CDN dependent immune clearance of tumors depends on cross talk or additive effects of both bone marrow and stromal cells. Indeed, both STING $^{-/-}$ \rightarrow WT and WT \rightarrow STING $^{-/-}$ animals experience delayed tumor outgrowth after CDN treatment. Similarly, using a series of bone marrow chimeras with TNF α protein knockouts, we showed that both WT \rightarrow TNF α $^{-/-}$ and TNF α $^{-/-}$ \rightarrow WT animals show some tumor clearance and injection site necrosis. However, bone marrow derived cells seem to be making the majority of TNF α because only in animals with TNF α competent bone marrow do we find TNF α in the TME.

We conclude that the tumor stroma is an important factor to consider when approaching any tumor therapy, especially those that utilize direct intratumoral injection of adjuvant. CDN injection acutely leads to the activation of the stroma, an inflammatory immune environment, and tumor clearance. Long term studies will need to be performed

to understand if this inflammatory environment persists, and if this is an ideal environment for the priming of adaptive immunity. We also look forward to understanding the long term effects of neutrophil and macrophage infiltration into the tumor site and into the tumor draining lymph node, because while these subsets are acutely inflammatory, it is understood that myeloid subsets can often be, or become immune suppressive. However, our observations of activated APC and long term vitiligo and dermatitis (unpublished) lead us to believe that these responses do exist and are potent, so we propose that IT CDN are a potent tool that represent the successful reinvigoration of a concept dating back to William Coley, one of the first men to experiment with tumor immunotherapy.

Drawbacks

There are several drawbacks of these studies, as indeed there are with any body of work. The use of mouse models has been somewhat contentiously debated over the past years, and even the use of inbred mice strains has come into question. The basic fact that a very small fraction of therapies discovered in mice translate to human clinical trials gives scientists pause, rightly so, about the validity and importance of their work. It is, however, undeniable that the use of these model systems allows for a greater understanding of the human body because small animal systems are manipulatable. Knockout animals are indispensable to our field, and indeed we have used many genetically modified organisms in these studies. While outbred mice may represent the genetic diversity of the human race better than clonal inbred animals, the sample size required to do such studies with reasonable scientific precision makes that goal unrealistic. Thus, we have chosen mice and indeed mouse tumor models not because we

expect absolute fidelity between mice and humans, but because it gave us the ability to quickly and thoroughly explore the mechanisms behind tumor clearance and immune activation.

The second drawback of these experiments is the tumor model. While we have experimented and shown efficacy of our therapies in multiple models including B16F1 (melanoma), EL-4 (lymphoma), and CT26 (colon carcinoma), the vast majority of our studies have been performed in the highly aggressive and metastatic mouse melanoma model B16F10. B16F10 grows at an enormous rate, often killing animals within 3 weeks of implantation, depending on the initial implanted tumor burden. This aggressiveness is orders of magnitude higher than that observed in any tumor in humans. However, we chose this model for several reasons. Firstly, the potency of aCTLA-4 IgG2a is staggering. In most models we experimented with, it cures tumors as a single agent. In order to discover combinatorial efficacy, we needed an extremely aggressive model. Additionally, B16F10 mirrors the efficacy of immunotherapy more closely than many models. While the field is advancing, the highest rate of tumor control observed in the clinic has been 50-60 percent with PD-1, when patients are binned according to the biomarker PD-L1. B16F10 is a vastly uninfitrated tumor with no truly curative immunodominant epitopes and a highly immunosuppressive tumor microenvironment, and it is the combination of these factors that makes it representative of the majority of fatal tumors in the human population.

Lastly, the treatment schema for the administration of CDN is not entirely representative of what we expect to be administered in clinical trials. We administered 100ug of the compound ADU-S100. This is an amount that has been optimized for the

clearance of aggressive tumors through the formation of necrosis. We used this dose to understand the basis of this necrosis and to understand the ability of different cell types to contribute to it. However this dosage, as we have shown, is not optimal for the induction of a CD8+ t cell response. It is indeed toxic to TIL acutely. And while this does activate dendritic cells and induce long term immunity, our collaborators at Aduro Biotech have shown that lower doses allow for better long term immunity in less aggressive tumor models.

REFERENCES

1. McCarthy, E.F. The toxins of William B. Coley and the treatment of bone and soft-tissue sarcomas. *The Iowa orthopaedic journal* **26**, 154-158 (2006).
2. Gatti, R.A. & Good, R.A. OCCURRENCE OF MALIGNANCY IN IMMUNODEFICIENCY DISEASES - LITERATURE REVIEW. *Cancer* **28**, 89-& (1971).
3. Penn, I., Halgrims.Cg & Starzl, T.E. DE-NOVO MALIGNANT TUMORS IN ORGAN TRANSPLANT RECIPIENTS. *Transplantation Proceedings* **3**, 773-& (1971).
4. Shankaran, V., *et al.* IFN gamma and lymphocytes prevent primary tumour development and shape tumour immunogenicity. *Nature* **410**, 1107-1111 (2001).
5. Dong, H., *et al.* CD27 Stimulation Promotes the Frequency of IL-7 Receptor-Expressing Memory Precursors and Prevents IL-12-Mediated Loss of CD8(+) T Cell Memory in the Absence of CD4(+) T Cell Help. *Journal of Immunology* **188**, 3829-3838 (2012).
6. Freeman, G.J., *et al.* STRUCTURE, EXPRESSION, AND T-CELL COSTIMULATORY ACTIVITY OF THE MURINE HOMOLOG OF THE HUMAN LYMPHOCYTE-B ACTIVATION ANTIGEN-B7. *Journal of Experimental Medicine* **174**, 625-631 (1991).
7. Van Lier, R.A.W., *et al.* TISSUE DISTRIBUTION AND BIOCHEMICAL AND FUNCTIONAL PROPERTIES OF TP55 CD27 A NOVEL T CELL DIFFERENTIATION ANTIGEN. *Journal of Immunology* **139**, 1589-1596 (1987).
8. Boise, L.H., *et al.* CD28 Costimulation Can Promote T Cell Survival by Enhancing the Expression of Bcl-x(L) (Reprinted from Immunity, vol 3, pg 87-98, 1995). *Journal of Immunology* **185**, 3788-3799 (2010).
9. Croft, M. Co-stimulatory members of the TNFR family: Keys to effective T-cell immunity? *Nature Reviews Immunology* **3**, 609-620 (2003).
10. Welten, S.P.M., *et al.* CD27-CD70 Costimulation Controls T Cell Immunity during Acute and Persistent Cytomegalovirus Infection. *Journal of Virology* **87**, 6851-6865 (2013).
11. Brahmer, J.R., *et al.* Safety and Activity of Anti-PD-L1 Antibody in Patients with Advanced Cancer. *New England Journal of Medicine* **366**, 2455-2465 (2012).

12. Deng, L.F., *et al.* Irradiation and anti-PD-L1 treatment synergistically promote antitumor immunity in mice. *Journal of Clinical Investigation* **124**, 687-695 (2014).
13. Keir, M.E., Butte, M.J., Freeman, G.J. & Sharpe, A.H. PD-1 and its ligands in tolerance and immunity. *Annual Review of Immunology* **26**, 677-704 (2008).
14. Zinselmeyer, B.H., *et al.* PD-1 promotes immune exhaustion by inducing antiviral T cell motility paralysis. *Journal of Experimental Medicine* **210**, 757-774 (2013).
15. Darrah, P.A., *et al.* Multifunctional T(H)1 cells define a correlate of vaccine-mediated protection against *Leishmania major*. *Nature Medicine* **13**, 843-850 (2007).
16. Fowell, D. & Mason, D. EVIDENCE THAT THE T-CELL REPERTOIRE OF NORMAL RATS CONTAINS CELLS WITH THE POTENTIAL TO CAUSE DIABETES - CHARACTERIZATION OF THE CD4+ T-CELL SUBSET THAT INHIBITS THIS AUTOIMMUNE POTENTIAL. *Journal of Experimental Medicine* **177**, 627-636 (1993).
17. Hori, S., Nomura, T. & Sakaguchi, S. Control of regulatory T cell development by the transcription factor Foxp3. *Science* **299**, 1057-1061 (2003).
18. Sakaguchi, S., Sakaguchi, N., Asano, M., Itoh, M. & Toda, M. IMMUNOLOGICAL SELF-TOLERANCE MAINTAINED BY ACTIVATED T-CELLS EXPRESSING IL-2 RECEPTOR ALPHA-CHAINS (CD25) - BREAKDOWN OF A SINGLE MECHANISM OF SELF-TOLERANCE CAUSES VARIOUS AUTOIMMUNE-DISEASES. *Journal of Immunology* **155**, 1151-1164 (1995).
19. Bennett, C.L., *et al.* The immune dysregulation, polyendocrinopathy, enteropathy, X-linked syndrome (IPEX) is caused by mutations of FOXP3. *Nature Genetics* **27**, 20-21 (2001).
20. Joetham, A., *et al.* Naturally occurring lung CD4(+) CD25(+) T cell regulation of airway allergic responses depends on IL-10 induction of TGF-beta. *Journal of Immunology* **178**, 1433-1442 (2007).
21. Pandiyan, P., Zheng, L.X., Ishihara, S., Reed, J. & Lenardo, M.J. CD4(+) CD25(+) Foxp3(+) regulatory T cells induce cytokine deprivation -mediated apoptosis of effector CD4(+) T cells. *Nature Immunology* **8**, 1353-1362 (2007).
22. Vignali, D.A.A., Collison, L.W. & Workman, C.J. How regulatory T cells work. *Nature Reviews Immunology* **8**, 523-532 (2008).
23. Sakaguchi, S., Yamaguchi, T., Nomura, T. & Ono, M. Regulatory T cells and immune tolerance. *Cell* **133**, 775-787 (2008).

24. Tadokoro, C.E., *et al.* Regulatory T cells inhibit stable contacts between CD4(+) T cells and dendritic cells in vivo. *Journal of Experimental Medicine* **203**, 505-511 (2006).
25. Bettini, M.L. & Vignali, D.A.A. Development of thymically derived natural regulatory T cells. in *Year in Immunology 2*, Vol. 1183 (ed. Rose, N.R.) 1-12 (Wiley-Blackwell, Malden, 2010).
26. Yadav, M., Stephan, S. & Bluestone, J.A. Peripherally induced Tregs - role in immune homeostasis and autoimmunity. *Frontiers in Immunology* **4**, 12 (2013).
27. Li, M.O., Sanjabi, S. & Flavell, R.A. Transforming growth factor-beta controls development, homeostasis, and tolerance of T cells by regulatory T cell-dependent and -independent mechanisms. *Immunity* **25**, 455-471 (2006).
28. Duraiswamy, J., Kaluza, K.M., Freeman, G.J. & Coukos, G. Dual Blockade of PD-1 and CTLA-4 Combined with Tumor Vaccine Effectively Restores T-Cell Rejection Function in Tumors. *Cancer Research* **73**, 3591-3603 (2013).
29. Keenan, B.P., *et al.* A Listeria Vaccine and Depletion of T-Regulatory Cells Activate Immunity Against Early Stage Pancreatic Intraepithelial Neoplasms and Prolong Survival of Mice. *Gastroenterology* **146**, 1784-+ (2014).
30. Peggs, K.S., Quezada, S.A., Chambers, C.A., Korman, A.J. & Allison, J.P. Blockade of CTLA-4 on both effector and regulatory T cell compartments contributes to the antitumor activity of anti-CTLA-4 antibodies. *Journal of Experimental Medicine* **206**, 1717-1725 (2009).
31. Simpson, T.R., *et al.* Fc-dependent depletion of tumor-infiltrating regulatory T cells co-defines the efficacy of anti-CTLA-4 therapy against melanoma. *Journal of Experimental Medicine* **210**, 1695-1710 (2013).
32. Curran, M.A., Montalvo, W., Yagita, H. & Allison, J.P. PD-1 and CTLA-4 combination blockade expands infiltrating T cells and reduces regulatory T and myeloid cells within B16 melanoma tumors. *Proceedings of the National Academy of Sciences of the United States of America* **107**, 4275-4280 (2010).
33. Jenkins, M.K. & Schwartz, R.H. ANTIGEN PRESENTATION BY CHEMICALLY MODIFIED SPLENOCYTES INDUCES ANTIGEN-SPECIFIC T-CELL UNRESPONSIVENESS INVITRO AND INVIVO. *Journal of Experimental Medicine* **165**, 302-319 (1987).
34. Greenwald, R.J., Boussiotis, V.A., Lorschach, R.B., Abbas, A.K. & Sharpe, A.H. CTLA-4 regulates induction of anergy in vivo. *Immunity* **14**, 145-155 (2001).
35. Parry, R.V., *et al.* CTLA-4 and PD-1 receptors inhibit T-cell activation by distinct mechanisms. *Molecular and Cellular Biology* **25**, 9543-9553 (2005).

36. Collins, S., *et al.* Opposing regulation of T cell function by Egr-1/NAB2 and Egr-2/Egr-3. *European Journal of Immunology* **38**, 528-536 (2008).
37. Collins, S., *et al.* Regulation of CD4(+) and CD8(+) Effector Responses by Sprouty-1. *Plos One* **7**(2012).
38. Safford, M., *et al.* Egr-2 and Egr-3 are negative regulators of T cell activation. *Nature Immunology* **6**, 472-480 (2005).
39. Zheng, Y., *et al.* Egr2-dependent gene expression profiling and ChIP-Seq reveal novel biologic targets in T cell anergy (vol 55, pg 283, 2013). *Molecular Immunology* **56**, 530-530 (2013).
40. Goldberg, M.V., *et al.* Role of PD-1 and its ligand, B7-H1, in early fate decisions of CD8 T cells. *Blood* **110**, 186-192 (2007).
41. Grosso, J.F., *et al.* Functionally Distinct LAG-3 and PD-1 Subsets on Activated and Chronically Stimulated CD8 T Cells. *Journal of Immunology* **182**, 6659-6669 (2009).
42. Okazaki, T., Maeda, A., Nishimura, H., Kurosaki, T. & Honjo, T. PD-1 immunoreceptor inhibits B cell receptor-mediated signaling by recruiting src homology 2-domain-containing tyrosine phosphatase 2 to phosphotyrosine. *Proceedings of the National Academy of Sciences of the United States of America* **98**, 13866-13871 (2001).
43. Woo, S.-R., *et al.* Immune Inhibitory Molecules LAG-3 and PD-1 Synergistically Regulate T-cell Function to Promote Tumoral Immune Escape. *Cancer Research* **72**, 917-927 (2012).
44. Fourcade, J., *et al.* PD-1 and Tim-3 Regulate the Expansion of Tumor Antigen-Specific CD8+ T Cells Induced by Melanoma Vaccines. *Cancer Research* **74**, 1045-1055 (2014).
45. Topalian, S.L., *et al.* Safety, Activity, and Immune Correlates of Anti-PD-1 Antibody in Cancer. *New England Journal of Medicine* **366**, 2443-2454 (2012).
46. Wolchok, J.D., *et al.* Nivolumab plus Ipilimumab in Advanced Melanoma. *New England Journal of Medicine* **369**, 122-133 (2013).
47. Tivol, E.A., *et al.* LOSS OF CTLA-4 LEADS TO MASSIVE LYMPHOPROLIFERATION AND FATAL MULTIORGAN TISSUE DESTRUCTION, REVEALING A CRITICAL NEGATIVE REGULATORY ROLE OF CTLA-4. *Immunity* **3**, 541-547 (1995).
48. Linsley, P.S., *et al.* HUMAN B7-1 (CD80) AND B7-2 (CD86) BIND WITH SIMILAR AVIDITIES BUT DISTINCT KINETICS TO CD28 AND CTLA-4 RECEPTORS. *Immunity* **1**, 793-801 (1994).

49. Zhang, Y. & Allison, J.P. Interaction of CTLA-4 with AP50, a clathrin-coated pit adaptor protein. *Proceedings of the National Academy of Sciences* **94**, 9273-9278 (1997).
50. June, C.H., Bluestone, J.A., Nadler, L.M. & Thompson, C.B. THE B7 AND CD28 RECEPTOR FAMILIES. *Immunology Today* **15**, 321-331 (1994).
51. Contardi, E., *et al.* CTLA-4 is constitutively expressed on tumor cells and can trigger apoptosis upon ligand interaction. *International Journal of Cancer* **117**, 538-550 (2005).
52. Selby, M.J., *et al.* Anti-CTLA-4 Antibodies of IgG2a Isotype Enhance Antitumor Activity through Reduction of Intratumoral Regulatory T Cells. *Cancer Immunology Research* **1**, 32-42 (2013).
53. Hayashi, F., *et al.* The innate immune response to bacterial flagellin is mediated by Toll-like receptor 5. *Nature* **410**, 1099-1103 (2001).
54. Hoshino, K., *et al.* Cutting edge: Toll-like receptor 4 (TLR4)-deficient mice are hyporesponsive to lipopolysaccharide: Evidence for TLR4 as the Lps gene product. *Journal of Immunology* **162**, 3749-3752 (1999).
55. O'Neill, L.A.J., Golenbock, D. & Bowie, A.G. The history of Toll-like receptors - redefining innate immunity. *Nature Reviews Immunology* **13**, 453-460 (2013).
56. Akira, S. & Takeda, K. Toll-like receptor signalling. *Nature Reviews Immunology* **4**, 499-511 (2004).
57. Sun, L., Wu, J., Du, F., Chen, X. & Chen, Z.J. Cyclic GMP-AMP Synthase Is a Cytosolic DNA Sensor That Activates the Type I Interferon Pathway. *Science* **339**, 786-791 (2013).
58. Ablasser, A., *et al.* cGAS produces a 2'-5'-linked cyclic dinucleotide second messenger that activates STING. *Nature* **498**, 380-+ (2013).
59. Barber, G.N. STING-dependent cytosolic DNA sensing pathways. *Trends in Immunology* **35**, 88-93 (2014).
60. Jin, L., *et al.* MPYS, a novel membrane tetraspanner, is associated with major histocompatibility complex class II and mediates transduction of apoptotic signals. *Molecular and Cellular Biology* **28**, 5014-5026 (2008).
61. Ishikawa, H. & Barber, G.N. Sting is an endoplasmic reticulum adaptor that facilitates innate immune signaling. *Cytokine* **48**, 128-128 (2009).
62. Sun, W.X., *et al.* ERIS, an endoplasmic reticulum IFN stimulator, activates innate immune signaling through dimerization. *Proceedings of the National Academy of Sciences of the United States of America* **106**, 8653-8658 (2009).

63. Konno, H., Konno, K. & Barber, G.N. Cyclic Dinucleotides Trigger ULK1 (ATG1) Phosphorylation of STING to Prevent Sustained Innate Immune Signaling. *Cell* **155**, 688-698 (2013).
64. Konno, H., Ishikawa, H., Ma, Z. & Barber, G.N. Sting regulates intracellular DNA-mediated, type I interferon-dependent innate immunity. *Cytokine* **52**, 61-62 (2010).
65. Sauer, J.D., *et al.* The N-Ethyl-N-Nitrosourea-Induced Goldenticket Mouse Mutant Reveals an Essential Function of Sting in the In Vivo Interferon Response to *Listeria monocytogenes* and Cyclic Dinucleotides. *Infection and Immunity* **79**, 688-694 (2011).
66. Jin, L., *et al.* MPYS Is Required for IFN Response Factor 3 Activation and Type I IFN Production in the Response of Cultured Phagocytes to Bacterial Second Messengers Cyclic-di-AMP and Cyclic-di-GMP. *Journal of Immunology* **187**, 2595-2601 (2011).
67. Yang K, W.J., Wu M, Li M, Wang Y, Huang X. Mesenchymal stem cells detect and defend against gammaherpesvirus infection via the cGAS-STING pathway. . Vol. 5 (Scientific Reports, 2015).
68. Chen, H.H., *et al.* Activation of STAT6 by STING Is Critical for Antiviral Innate Immunity. *Cell* **147**, 436-446 (2011).
69. Sun, L., *et al.* Coronavirus Papain-like Proteases Negatively Regulate Antiviral Innate Immune Response through Disruption of STING-Mediated Signaling. *Plos One* **7**(2012).
70. Sze, A., *et al.* Host Restriction Factor SAMHD1 Limits Human T Cell Leukemia Virus Type 1 Infection of Monocytes via STING-Mediated Apoptosis. *Cell Host & Microbe* **14**, 422-434 (2013).
71. Dai, P.H., *et al.* Modified Vaccinia Virus Ankara Triggers Type I IFN Production in Murine Conventional Dendritic Cells via a cGAS/STING-Mediated Cytosolic DNA-Sensing Pathway. *Plos Pathogens* **10**, 13 (2014).
72. Guo, H.T., *et al.* NLRX1 Sequesters STING to Negatively Regulate the Interferon Response, Thereby Facilitating the Replication of HIV-1 and DNA Viruses. *Cell Host & Microbe* **19**, 515-528 (2016).
73. Trotard, M., *et al.* Sensing of HIV-1 Infection in Tzm-bl Cells with Reconstituted Expression of STING. *Journal of Virology* **90**, 2064-2076 (2016).
74. Chen, Q., *et al.* Carcinoma-astrocyte gap junctions promote brain metastasis by cGAMP transfer. *Nature* **533**, 493-+ (2016).

75. Ablasser, A., *et al.* Cell intrinsic immunity spreads to bystander cells via the intercellular transfer of cGAMP. *Nature* **503**, 530-+ (2013).
76. Huang, L., *et al.* Cutting Edge: DNA Sensing via the STING Adaptor in Myeloid Dendritic Cells Induces Potent Tolerogenic Responses. *Journal of Immunology* **191**, 3509-3513 (2013).
77. Archer, K.A., Durack, J. & Portnoy, D.A. STING-Dependent Type I IFN Production Inhibits CellMediated Immunity to *Listeria monocytogenes*. *Plos Pathogens* **10**(2014).
78. Vaure, C. & Liu, Y.Q. A comparative review of toll-like receptor 4 expression and functionality in different animal species. *Frontiers in Immunology* **5**, 15 (2014).
79. da Conceicao, T.M., *et al.* Essential role of RIG-I in the activation of endothelial cells by dengue virus. *Virology* **435**, 281-292 (2013).
80. Ranta, V., *et al.* Human vascular endothelial cells produce tumor necrosis factor-alpha in response to proinflammatory cytokine stimulation. *Critical Care Medicine* **27**, 2184-2187 (1999).
81. McClure, R. & Massari, P. TLR-dependent human mucosal epithelial cell responses to microbial pathogens. *Frontiers in Immunology* **5**, 1-13 (2014).
82. Pardoll, D.M. The blockade of immune checkpoints in cancer immunotherapy. *Nature Reviews Cancer* **12**, 252-264 (2012).
83. Grosso, J.F., *et al.* LAG-3 regulates CD8+T cell accumulation and effector function in murine self- and tumor-tolerance systems. *Journal of Clinical Investigation* **117**, 3383-3392 (2007).
84. Chemnitz, J.M., Parry, R.V., Nichols, K.E., June, C.H. & Riley, J.L. SHP-1 and SHP-2 Associate with Immunoreceptor Tyrosine-Based Switch Motif of Programmed Death 1 upon Primary Human T Cell Stimulation, but Only Receptor Ligation Prevents T Cell Activation. *The Journal of Immunology* **173**, 945-954 (2004).
85. Li, J., *et al.* PD-1/SHP-2 Inhibits Tc1/Th1 Phenotypic Responses and the Activation of T Cells in the Tumor Microenvironment. *Cancer Research* **75**, 508-518 (2015).
86. Yokosuka, T., *et al.* Programmed cell death 1 forms negative costimulatory microclusters that directly inhibit T cell receptor signaling by recruiting phosphatase SHP2. *The Journal of Experimental Medicine* **209**, 1201-1217 (2012).

87. Yasukawa, H., Sasaki, A. & Yoshimura, A. Negative regulation of cytokine signaling pathways. *Annual Review of Immunology* **18**, 143-164 (2000).
88. Hanada, T. & Yoshimura, A. Regulation of cytokine signaling and inflammation. *Cytokine & Growth Factor Reviews* **13**, 413-421 (2002).
89. Nirschl, C.J. & Drake, C.G. Molecular Pathways: Coexpression of Immune Checkpoint Molecules: Signaling Pathways and Implications for Cancer Immunotherapy. *Clinical Cancer Research* **19**, 4917-4924 (2013).
90. Hirano, F., *et al.* Blockade of B7-H1 and PD-1 by monoclonal antibodies potentiates cancer therapeutic immunity. *Cancer Research* **65**, 1089-1096 (2005).
91. Twyman-Saint Victor, C., *et al.* Radiation and dual checkpoint blockade activate non-redundant immune mechanisms in cancer. *Nature* **520**, 373-+ (2015).
92. Le, D.T., *et al.* Safety and Survival With GVAX Pancreas Prime and Listeria Monocytogenes-Expressing Mesothelin (CRS-207) Boost Vaccines for Metastatic Pancreatic Cancer. *Journal of Clinical Oncology* **33**, 1325-+ (2015).
93. Brockstedt, D.G., *et al.* Listeria-based cancer vaccines that segregate immunogenicity from toxicity. *Proceedings of the National Academy of Sciences of the United States of America* **101**, 13832-13837 (2004).
94. Woodward, J.J., Iavarone, A.T. & Portnoy, D.A. c-di-AMP Secreted by Intracellular Listeria monocytogenes Activates a Host Type I Interferon Response. *Science* **328**, 1703-1705 (2010).
95. Chandra, D., *et al.* STING Ligand c-di-GMP Improves Cancer Vaccination against Metastatic Breast Cancer. *Cancer immunology research* **2**, 901-910 (2014).
96. Baird, J.R., *et al.* Radiotherapy Combined with Novel STING-Targeting Oligonucleotides Results in Regression of Established Tumors. *Cancer Research* **76**, 50-61 (2016).
97. Lizotte, P.H., *et al.* Attenuated Listeria monocytogenes reprograms M2-polarized tumor-associated macrophages in ovarian cancer leading to iNOS-mediated tumor cell lysis. *Oncoimmunology* **3**, 12 (2014).
98. Lim, J.Y.H., Brockstedt, D.G., Lord, E.M. & Gerber, S.A. Radiation therapy combined with Listeria monocytogenes-based cancer vaccine synergize to enhance tumor control in the B16 melanoma model. *Oncoimmunology* **3**(2014).
99. Ralph, C., *et al.* Modulation of Lymphocyte Regulation for Cancer Therapy: A Phase II Trial of Tremelimumab in Advanced Gastric and Esophageal Adenocarcinoma. *Clinical Cancer Research* **16**, 1662-1672 (2010).

100. Dahan, R., *et al.* Fc gamma Rs Modulate the Anti-tumor Activity of Antibodies Targeting the PD-1/PD-L1 Axis. *Cancer Cell* **28**, 285-295 (2015).
101. Nimmerjahn, F. & Ravetch, J.V. Fc gamma receptors as regulators of immune responses. *Nature Reviews Immunology* **8**, 34-47 (2008).
102. Downey, C.M., Aghaei, M., Schwendener, R.A. & Jirik, F.R. DMXAA Causes Tumor Site-Specific Vascular Disruption in Murine Non-Small Cell Lung Cancer, and like the Endogenous Non-Canonical Cyclic Dinucleotide STING Agonist, 2' 3'-cGAMP, Induces M2 Macrophage Repolarization. *Plos One* **9**, 14 (2014).
103. Dubensky, T.W., Jr., Kanne, D.B. & Leong, M.L. Rationale, progress and development of vaccines utilizing STING-activating cyclic dinucleotide adjuvants. *Therapeutic advances in vaccines* **1**, 131-143 (2013).
104. Fu, J., *et al.* STING agonist formulated cancer vaccines can cure established tumors resistant to PD-1 blockade. *Science Translational Medicine* **7**, 11 (2015).
105. Ohkuri, T., *et al.* STING Contributes to Antiglioma Immunity via Triggering Type I IFN Signals in the Tumor Microenvironment. *Cancer Immunology Research* **2**, 1199-1208 (2014).
106. Chandra, D., *et al.* STING Ligand c-di-GMP Improves Cancer Vaccination against Metastatic Breast Cancer. *Cancer Immunology Research* **2**, 901-910 (2014).
107. Woo, S.R., *et al.* STING-Dependent Cytosolic DNA Sensing Mediates Innate Immune Recognition of Immunogenic Tumors. *Immunity* **41**, 830-842 (2014).
108. Deng, L., *et al.* STING-Dependent Cytosolic DNA Sensing Promotes Radiation-Induced Type I Interferon-Dependent Antitumor Immunity in Immunogenic Tumors. *Immunity* **41**, 843-852 (2014).
109. Demaria, O., *et al.* STING activation of tumor endothelial cells initiates spontaneous and therapeutic antitumor immunity. *Proceedings of the National Academy of Sciences of the United States of America* **112**, 15408-15413 (2015).
110. Wajant, H., Pfizenmaier, K. & Scheurich, P. Tumor necrosis factor signaling. *Cell Death and Differentiation* **10**, 45-65 (2003).
111. Parham, P. (ed.) *The Immune System*, 51-55 (Garland Science, Taylor and Francis Group, 270 Madison Avenue, Ny, 2009).
112. van Horsen, R., ten Hagen, T.L.M. & Eggermont, A.M.M. TNF-alpha in cancer treatment: Molecular insights, antitumor effects, and clinical utility. *Oncologist* **11**, 397-408 (2006).

113. Bashir, M.M., Sharma, M.R. & Werth, V.P. TNF-alpha production in the skin. *Archives of Dermatological Research* **301**, 38-38 (2009).
114. Botero, J.E., Contreras, A. & Parra, B. Profiling of inflammatory cytokines produced by gingival fibroblasts after human cytomegalovirus infection. *Oral Microbiology and Immunology* **23**, 291-298 (2008).
115. Wu, J. & Chen, Z.J. Innate Immune Sensing and Signaling of Cytosolic Nucleic Acids. *Annual Review of Immunology, Vol 32* **32**, 461-488 (2014).
116. Wang, W.S., *et al.* PD1 blockade reverses the suppression of melanoma antigen-specific CTL by CD4(+)CD25(Hi) regulatory T cells. *International Immunology* **21**, 1065-1077 (2009).

CURRICULUM VITAE

Brian Francica

Addresses:

brianfrancica@gmail.com

Home: 1707 Lancaster St., Baltimore, MD, 21231

(256) 975-1661

Work: CRB1 Room 416, 1550 Orleans St, Baltimore, MD, 21231

(401) 502-9778

Education:

Johns Hopkins University, Baltimore, MD

Doctor of Philosophy, May 2016

Immunology Training Program, Johns Hopkins School of Medicine

Focus: Tumor immunology, adaptive and innate immune responses to vaccination

The University of Virginia, Charlottesville, Virginia

Bachelor of Science, May 2011

College of Arts and Science

Major: Bachelor of Science in Biological Sciences

Virgil I. Grissom High School, Huntsville, Alabama

Advanced Diploma, May 2007

Medical Research Experience:

Ph.D. Candidate, Johns Hopkins University School of Medicine

August 2011- Present

Co- Mentors Charles G. Drake M.D., Ph.D., Co-Director Cancer Immunology and Hematopoiesis

Program, Professor of Oncology, and Drew M. Pardoll M.D., Ph.D., Co-Director, Cancer Immunology and

Hematopoiesis Program, Professor of Oncology

- Performed independent research in multiple divisions of immunology.
 - Investigated genetic profiles of T-cell tolerance through microarray analysis
 - Explored the efficacy of genetically engineered *Listeria Monocytogenes* to generate and maintain anti-tumor immunity
 - Studied the innate and adaptive immune effects of the neo-adjuvant cyclic dinucleotide

- Mastered wide range of immunological, microbiological, cell biological and imaging techniques.
 - Mouse dissection and tissue preparation, human tissue preparation, 12+ color flow cytometry, ELISA, plasmid or lentiviral transfection/transduction, microscopy, western blot, etc.
- Developed and refined *in vivo* and *in vitro* assays for anti-tumor immunity and T-cell cytolytic activity.
 - Preclinical tumor models such as B16 (F1,F10), CT26, and MC38.
 - Generation and maintenance of bone marrow chimeras and other mouse models
 - T cell magnetic bead enrichment and adoptive transfer techniques
 - *In vitro and in vivo* CD8+ T cell killing, Tregulatory/Teffector suppression assays
- Supervised and mentored several junior students in experimental techniques, critical analysis, and the scientific method.
- Participated in scientific collaborations with biotechnological companies as well as pharmaceutical companies.
- Received NIH training grant for student training, Keystone Travel Grant for Students with outstanding abstract submissions, and the Cancer Research Institute Fellowship.
- Selected for oral as well as poster presentations at Cancer Research Institute and Keystone Immunology conferences.
- 3 manuscripts in preparation.

Undergraduate Researcher and Research Specialist, University of Virginia

May 2009 – August 2011

Timothy Bullock, Ph.D., Principle Investigator, Associate Professor of Pathology

- Performed independent research investigating the use of adjuvants to elicit competent dendritic cell licensing, effective adaptive immune responses, and tumor clearance.
- Learned a variety of immunological assays and developed *in vivo* and *in vitro* experimental assays.
- Presented research findings to departmental faculty in oral, poster and written formats.

Undergraduate Researcher and Research Specialist, University of Virginia

Fall 2008 – Spring 2009

Raymond Keller, Ph.D., Principle Investigator, Department of Biological Sciences

David Shook, Ph.D., Research Scientist, Department of Biological Sciences

- Performed directed and independent research investigating the development of *Xenopus Laevis* blastula formation and kinetic forces that shape development.
- Presented research findings to departmental faculty in oral, poster, and written formats.

Research Grants and Honors:

Recipient, Training Grant in Cellular and Molecular National Institutes of Health, T32-AI007247-33 August 2008 – July 2010

Recipient, 1st Place August- 2015
Johns Hopkins Medical and Educational Perspectives (MEP) Case Competition
Biotechnology Entrepreneurship Symposium

Recipient, Keystone Travel Grant for Outstanding Abstracts
December 2015

Recipient, Award for Outstanding Poster Presentation
Johns Hopkins Immunology Conference October 2015

Community Involvement and Professional Development:

Teaching Assistant, Johns Hopkins University, Department of Immunology
Taught Graduate Immunology, Senior TA in 2016 February 2013-2016

Graduate Student Liaison- Johns Hopkins University to Milford Mill Academy
Spring 2016

Selected Conference Abstracts and Presentations:

Francica BJ, Ghasemzadeh A, Dubensky TW, and Drake CG. Radio-resistant Stromal Cells Initiate the Innate Response to Cyclic Dinucleotides. Keystone Symposia, Cancer Vaccines: Targeting Cancer Genes for Immunotherapy 2016. Whistler, BC, Canada. March 7, 2016. (oral presentation and poster presentation)

Francica BJ, Ghasemzadeh A, Dubensky TW, Brockstedt DG, Lauer P, Korman A, Selby M, Pardoll DM, and Drake CG. Combinatorial Listeria+Depleting Antibody Cures Established B16 Melanoma. Keystone Symposia, Tumor Immunology: Multidisciplinary Science Driving Combination Therapy 2015. Banff, AB, Canada. February 8, 2015. (poster presentation)

Francica BJ, Nirschl CJ, Ceccato CM, Nirschl TR, and Drake CG. Adoptive Transfer Therapy is Greatly Improved by an Engineered Listeria Vaccine Targeting Shared Human and Mouse Antigens. Cancer Research Institute, Cancer Immunotherapy 2014: Out of the Gate. New York, New York. October 6, 2014. (poster presentation)

Manuscripts in Preparation:

Francica BJ, Ghasemzadeh A, Kochel CM, Nirschl TR, Theodros D, Nirschl CJ, Marsicano A, Dubensky TW, Korman A, Selby M, Pardoll DM, and Drake CG. Combination Listeria Vaccine + Checkpoint Blockade Effectively Reduces Tumor Burden of Established B16F10 Melanoma in an Fc-Dependent Manner. *Manuscript in preparation.*

Francica BJ, Ghasemzadeh A, Marciscano A, Theodros D, Nirschl TR, Dubensky TW, Pardoll DM, and Drake CG. Radio Resistant Stromal Cells Initiate the Innate Response to Cyclic Dinucleotide Therapy. *Manuscript in preparation.*

Francica BJ, Nirschl CJ, Goldberg MV, Huang DD, and Drake CG. Independent Control of PD-1 and Egr2 in Models of CD8+ T-Cell Tolerance. *Manuscript in preparation.*

Selected Publications:

Jackson CM, Kochel CM, Nirschl CJ, Durham NM, Ruzevick J, Alme A, **Francica BJ**, Elias J, Daniels A, Dubensky TW Jr, Lauer P, Brockstedt DG, Baxi EG, Calabresi PA, Taube JM, Pardo CA, Brem H, Pardoll DM, Lim M, Drake CG. Systemic Tolerance Mediated by Melanoma Brain Tumors Is Reversible by Radiotherapy and Vaccination. *Clin Cancer Res.* 2015 Oct 21.

Martin AM, Nirschl TR, Nirschl CJ, **Francica BJ**, Kochel CM, van Bokhoven A, Meeker AK, Lucia MS, Anders RA, DeMarzo AM and Drake CG. Paucity of PD-L1 expression in prostate cancer: innate and adaptive immune resistance. *Prostate Cancer and Prostatic Diseases* 18, 325-332. December 2015.

Sharabi AB, Nirschl CJ, Kochel CM, Nirschl TR, **Francica BJ**, Velarde E, Deweese TL, Drake CG. Stereotactic Radiation Therapy Augments Antigen-Specific PD-1-Mediated Antitumor Immune Responses via Cross-Presentation of Tumor Antigen. *Cancer Immunology Research.* April 2015.